TOP SECRET

NO FOREIGN DISSEMINATION

[redacted]

14 00039104D

# PERFORMANCE ANALYSIS FOR THE 1102 SYSTEM

3 JUNE 1968

CONTRIBUTORS: [redacted]

Declassified and Released by the N R O

In Accordance with E. O. 12958

on NOV 26 1997

TOP SECRET

NO FOREIGN DISSEMINATION

HANDLE VIA
TALENT-KEYHOLE
CONTROL SYSTEM ONLY



[redacted]
Copy No. [redacted]

# PERFORMANCE ANALYSIS FOR THE 1102 SYSTEM

3 JUNE 1968

CONTRIBUTORS: [redacted]

Itek OPTICAL SYSTEMS DIVISION
ITEK CORPORATION • 10 MAGUIRE ROAD • LEXINGTON, MASSACHUSETTS 02173

[redacted]



~~TOP SECRET~~
~~NO FOREIGN DISSEMINATION~~

CONTENTS

TABLES

# 1. SUMMARY

The performance of the 1102 system was generally excellent. The following paragraphs regarding the performance of the panoramic cameras have been quoted from the PEIR Report* on mission 1102.

"The PET group and photointerpreters agree that the best photography of mission 1102 is better than any previous KH-4 photography. The performance of the forward-looking camera appears to be slightly better than the aft-looking camera, . . . Nine mobile and fixed CORN targets were recorded. The best targets observed in the original negative yielded approximately six feet ground resolved distance along the line of flight (FMC direction) and seven feet across the line of flight (scan direction) for the aft-looking camera; the forward-looking camera yielded approximately six feet in both directions. Several very favorable factors combined to produce the best KH-4 mission to date. The primary factors were good atmospheric conditions, increased scale through lower altitude and improved camera performance." However, all mission conditions were not ideal. The mission took place in the middle of the winter, and, due to low solar altitudes in the northern hemisphere, it was necessary to use longer exposure times. The maximum slit was used extensively during the mission in the forward-looking camera, and a rather large slit (0.270 inch) was used most of the time in the aft-looking camera. Thus, the camera performance, especially in the forward-looking camera, was limited by image smear, and mission 1102 should be considered as a rather severe test of the panoramic cameras under large smear conditions. Hence, the mission 1102 photography, though admittedly better than any previous KH-4 photography, does not approach the upper limit of the performance capability of the 1100 series panoramic cameras.

The performance analysis of mission 1102 has not only established the factors that controlled this system's performance, but also shows the steps that are required to improve the performance of the camera system. Specific recommendations for this purpose are presented in Section 6 of this report.

The most important conclusion of the 1102 performance analysis report is that image smear was a significant degrading factor. Thus, in order to optimize the system performance, it is essential that image smear be considerably reduced. Otherwise, for missions of prevailing low solar altitudes, the high performance of the third generation lenses could be nullified by image smear. Therefore, if image smear is reduced to a reasonably small magnitude, it should be possible for some of the future missions to achieve a ground resolved distance of less than 5 feet.

Section 3.4 of this report is a comparative study of how the performance of the 1102 system would have been affected by variations in the system parameters. This section is illuminating because it shows the steps that are required to optimize the system performance and is the basis of the recommendations of Section 6. The most important conclusion of Section 3.4 is that

---

[redacted]

significant gains in improved performance can be attained by reducing the average image smear present in the 1102 system. However, it is not necessary to eliminate image smear altogether because near optimum performance can be obtained with 3 to 4 microns of residual image smear. Section 3.4 also shows that a gain in resolution can be obtained by reducing the average altitude of operation to 80 nm. For mission 1102, the average altitude was 87.6 nm.

## 2. INTRODUCTION

It has already been mentioned in the summary that mission 1102 produced some excellent photography, and it is generally agreed that the mission 1102 photography was superior to the photography of mission 1101. To a great extent the improvement was a result of better focusing of the 1102 system panoramic cameras. The focusing technique was described in detail in the 1101 performance analysis report,* and it was shown that uncertainties about the vacuum peak focus position exist because the panoramic cameras are focused in air. Of course, all the focusing difficulties could be eliminated entirely by focusing the cameras dynamically in vacuum. The accuracy of the presently utilized focusing technique is affected by various factors, the most important of which are knowledge of the air-to-vacuum focus shift of each Petzval lens and barometric pressure. In order to reduce any possible errors in focusing, the barometric pressure under which the focusing tests are performed is being recorded, and extensive thermal and vacuum focus tests were performed on a second and a third generation Petzval lens at the contractor's facility. These tests showed that the air-to-vacuum focus shift is approximately 0.014 to 0.0145 inch. Even with these refinements, the presently utilized focusing technique may occasionally produce an accumulated focusing error of 0.001 inch. Such a deviation from the peak focus position will have a serious degrading effect on a third generation lens.

When the 1102 system was being focused, the results of the vacuum-to-air focus shift tests conducted in the contractor's TORF chamber† were not yet available. Thus, a 0.015-inch vacuum-to-air focus shift was accepted based on the recomputation of the theoretical focus shift utilizing measured lens parameters. However, for an added measure of safety, the 1102 panoramic cameras were focused slightly off their respective peaks, which were compatible with an air-to-vacuum focus shift of 0.015 inch. Effectively, they were focused as if the anticipated air-to-vacuum focus shift was 0.0130 and 0.0125 inch for the forward- and aft-looking cameras, respectively. The 1101 cameras had been focused for an anticipated air-to-vacuum focus shift of 0.016 inch. Thus, the 1102 camera focusing represents a slight overcorrection of the 1101 camera focus conditions.‡ As a result of the way the 1102 cameras were focused in the laboratory, the forward-looking camera during the mission operated 0.0010 inch off its peak focus position, while the aft-looking camera operated 0.0015 inch off its respective peak.

---

[redacted]

† Thermal Optical Research Facility (in vacuum).

‡ Section 3.2 describes the focus conditions more thoroughly.

A major part of the performance analysis study consists of computations of resolution predictions for the CORN* resolution targets and HPL† targets. These computations utilize data from the following set of sources:

1. Static resolution versus focus tests of the Petzval lenses
2. Final dynamic resolution versus focus tests of the respective cameras
3. Air-to-vacuum focus shift of 0.014 inch
4. Film flatness tests of the cameras
5. Dynamic resolution versus image smear tests for each camera
6. Mission ephemeris data
7. Camera scanning rates and slits during mission
8. Camera image smear tests
9. Temperature effects on film lift
10. Nominal vehicle performance data.

The data from sources 1 through 4 are reduced manually on a per target basis, and are utilized for determining the static resolution (no image smear) at the target image location on the panoramic format. The data of source 5 are also reduced manually. Sources 8, 9, and 10 are nominal system data. The data of sources 6 and 7 plus the results from all the other sources are combined together in a computer program from which ground resolved distances and other quantities are computed for each CORN or HPL target. For the CORN targets, a comparison between the predicted ground resolved distances and the actual readings has been provided in Section 3.3 of the report. Furthermore, in Appendix B, a statistical correlation is performed between the photo-interpreters ratings and the predicted ground resolved distances for HPL targets.

Other data that were examined in conjunction with mission 1102 are:

1. SRV tape recorder summary for mission 1102
2. Vehicle attitude data reduced from the stellar camera and supplied by NPIC‡
3. Image smear tests performed on unit no. 299§
4. Two reports on the thermal and vacuum tests of two Petzval lenses performed at the TORF chamber.

These data are examined in detail in Section 3.2.

---

*Controlled Range Network.
†High Priority Target List.
‡National Photographic Interpretation Center.
§Single panoramic camera used as a test bed.

# 3. SYSTEM PERFORMANCE

## 3.1 CORN TARGET RESOLUTION

Each CORN target deployed consisted of the 51/51 T-bar resolving power target, a Gray scale target, and 100-foot edge target. These targets have already been described in the mission 1101 performance analysis report,* so their description will not be repeated here. A more thorough explanation of these targets is also available in the CORN target manual.†

Table 3-1 lists the geographic distribution of the CORN targets deployed. Four were actually fixed targets (permanent installations). The first two columns labeled Pass and Frame uniquely identify the frame on which the image of a specific target display appears. The x and y coordinates listed in Table 3-1 pinpoint the position of the target image on the respective panoramic frame according to the universal grid system.

The images of the CORN and fixed targets were examined by a number of observers who determined the corresponding ground resolved distances.‡ The actual readings are shown in Table 3-2. Most of the readings were taken from the original negative except for the last few targets which were read from the first generation dupe positive (identified by an asterisk). The first number in each Reader column is the ground resolved distance in the along-track direction; the second number is the ground resolved distance in the cross-track direction.

## 3.2 DETERMINATION OF OPERATIONAL RESOLUTION

The method for determining the operational resolution is discussed more extensively in Section 3.2 of the 1101 performance analysis report. This technique is described only briefly in the present section.

The dynamic camera resolution, image smear, and static lens-film resolution for any image point are related by the expression:

$$R_d = \frac{R_s}{\left[1 + (bR_s)^{E_1}\right]^{E_2}} \tag{3.1}$$

where $R_d$ = dynamic camera resolution
$b$ = image smear
$R_s$ = static lens-film resolution
$E_1$ and $E_2$ = experimentally determined exponents

---

[redacted] Section 3.1.
† Controlled Range Network manual.
‡ In feet, equivalent to 1 bar and 1 space

Table 3-1 — CORN Target Coverage

| Pass | Frame | x | y | Location |
|---|---|---|---|---|
| 16 | 6 fwd | 20.4 | 3.7 | Edwards AFB, California; fixed target |
| | 12 aft | 56.0 | 2.8 | 34°51' N, 117°45' W |
| 32 | 13 fwd | 37.8 | 2.9 | Kingman, Arizona |
| | 19 aft | 37.9 | 3.1 | 35°15' N, 113°55' W |
| 48 | 21 fwd | 25.4 | 4.3 | Winslow, Arizona |
| | 27 aft | – | – | 35°1' N, 110°44' W |
| 48 | 48 fwd | 22.0 | 2.6 | Fort Huachuca, Arizona; fixed target |
| | 54 aft | 53.8 | 4.2 | 31°35' N, 110°18' W |
| 97 | 15 fwd | 56.1 | 1.8 | Palo Alto, California |
| | 21 aft | 19.1 | 5.2 | 37°25' N, 122°8' W |
| | 22 aft | 19.4 | 0.4 | |
| 113 | 24 fwd | 71.8 | 1.8 | Edwards AFB, California; fixed target |
| | 30 aft | 3.2 | 5.3 | 34°51' N, 117°45' W |
| 176 | 26 fwd | 23.6 | 3.1 | Wright Patterson AFB, Ohio; fixed target |
| | 32 aft | 52.3 | 4.3 | 39°46' N, 84°6' W |

Table 3-2 - Resolution Target Readings on Original Negative, feet

| | | Reader No. 1 | | Reader No. 2 | | Reader No. 3 | | Reader No. 4 | | Reader No. 5 | | Reader No. 6 | | Average | | |
|---|---|---|---|---|---|---|---|---|---|---|---|---|---|---|---|---|
| Pass | Frame | Along Track | Cross Track | Along Track | Cross Track | Along Track | Cross Track | Along Track | Cross Track | Along Track | Cross Track | Along Track | Cross Track | Along Track | Cross Track | Target Type |
| 16 | 6 fwd | 5.7 | 6.3 | 8 | 6.3 | 5.7 | 6.3 | 5.7 | 6.3 | 5.7 | 5.7 | 5.7 | 5.7 | 6.1 | 6.1 | Fixed, high contrast |
| 16 | 6 fwd | 7 | 8 | 9 | 9 | 6.3 | 8 | 8 | 8 | 9 | 8 | 7 | 6.3 | 7.7 | 7.9 | Fixed, medium contrast |
| 16 | 12 aft | 5.7 | 8 | 6.3 | 8 | 5.7 | 8 | 5.7 | 9 | 5.7 | 6.3 | 5.7 | 8 | 5.8 | 7.9 | Fixed, high contrast |
| 16 | 12 aft | 9 | 9 | 9 | 9 | 7.1 | 9 | 9 | 10 | 9 | 9 | 9 | 9 | 8.7 | 9.2 | Fixed, medium contrast |
| 32 | 13 fwd | 12 | 12 | 12 | 12 | 12 | 12 | 12 | 12 | 12 | 12 | 12 | 12 | 12 | 12 | CORN |
| 32 | 19 aft | 12 | 8 | 12 | 12 | 12 | 12 | 12 | 12 | 12 | 8 | 12 | 8 | 12 | 10 | CORN |
| 48 | 21 fwd | 12 | 16 | 12 | 16 | 12 | 16 | 12 | 16 | 12 | 12 | 12 | 16 | 12 | 15.3 | CORN |
| 48 | 48 fwd | 6.3 | 6.3 | 7 | 7 | 5.7 | 6.3 | 6.3 | 8 | 6.3 | 7 | 7 | 8 | 6.4 | 7.2 | Fixed, center leg |
| 48 | 48 fwd | 6.3 | 5.7 | 8 | 8 | 6.3 | 5.7 | 8 | 9 | 6.3 | 5.7 | 6.3 | 5.0 | 6.9 | 6.5 | Fixed, outer leg |
| 48 | 54 aft | 6.3 | 6.3 | 9 | 8 | 9 | 8 | 8 | 7 | 8 | 7 | 8 | 7 | 8.1 | 7.2 | Fixed |
| 97 | 15 fwd | 12 | 16 | 12 | 16 | 12 | 16 | 12 | 16 | 12 | 16 | 12 | 16 | 12 | 16 | CORN |
| 97 | 21 aft | 16 | 16 | 16 | 16 | 12 | 16 | 12 | 16 | 12 | 16 | 12 | 16 | 13.3 | 16 | CORN |
| 113* | 19 fwd | 16 | 16 | >16 | >16 | 16 | >16 | 16 | >16 | 16 | >16 | >16 | 16 | 16 | >16 | CORN |
| 113 | 26 aft | 12 | 16 | 16 | 16 | 16 | 16 | 16 | 16 | 16 | 16 | 16 | 16 | 15.3 | 16 | CORN |
| 113* | 24 fwd | 14 | 25 | - | - | 13 | 25 | 13 | 25 | 13 | 25 | 13 | 25 | 13.2 | 25 | Fixed |
| 113* | 30 aft | - | - | - | - | 18 | 14 | 16 | 18 | 18 | 14 | 18 | 20 | 17.5 | 16.5 | Fixed |
| 176* | 26 fwd | - | - | 11 | >16 | 11 | >16 | 11 | >16 | 11 | >16 | 11 | >16 | 11 | >16 | Fixed |
| 176* | 32 aft | 10 | >16 | 11 | >16 | 11 | >16 | 10 | >16 | 11 | >16 | 10 | >16 | 10.5 | >16 | Fixed |

*Dupe positive readings.

Exponents $E_1$ and $E_2$ were determined from resolution versus image smear tests performed at the contractor's laboratory. Table 3-3 shows the exponents that were determined for the 1102 forward- and aft-looking cameras. The static resolution, $R_s$, at a specific point of the panoramic format is dependent on the performance of the Petzval lens at the corresponding field angle, the focus position occupied by the film, and the film characteristics. Thus, for all practical purposes, $R_s$ varies over the panoramic format of a camera but is not a function of time (does not vary between successive frames). In fact, one could construct a contour map of $R_s$ over the panoramic format.

Table 3-3 — Mission 1102 Exponents

| Aft | | | Forward | |
|---|---|---|---|---|
| $E_1$ | $E_2$ | Contrast | $E_1$ | $E_2$ |
| 2.70 | 0.33 | Low 2:1 | 2.90 | 0.35 |
| 3.00 | 0.33 | High | 2.90 | 0.35 |

In the resolution predictions, the values of $R_s$ are determined individually for each target. To accomplish this, the static resolution of the lens as a function of field angle and focus position (from laboratory data) are utilized. For a specific target image, its y coordinate gives immediately the field angle the image occupies. In order to determine the focus position the same target image occupies, it is necessary to review the film flatness tests which provide the relative focus position of the target image with respect to the center of format. Finally, the operational focus position at the center of the format can be obtained from the final dynamic resolution versus focus tests performed at the contractor's laboratory. The results of these tests have been plotted in Figs. 3-1 through 3-4. The anticipated focus position at the center of format during the mission is also shown in these figures. Having determined the field angle and focus position of a specific target, the associated $R_s$ values are readily obtained.

The computation of image smear is also described in detail in Section 3.2 of the 1101 performance analysis report. Since it is not possible to compute the image smear exactly, a systematic image smear component, $b_s$, and a random component, $b_r$, are separately computed for each target image. Then, the total image smear, $b_t$, is determined by the equation

$$b_t = b_r + |b_s| \qquad (3.2)$$

$b_t$ is introduced into Equation (3.1) and utilized in the computation of the dynamic camera resolution, $R_d$. In turn, the ground resolved distance is related to $R_d$ by a scale factor affected by vehicle altitude, camera focal length, and location on the panoramic format of the target image. The ground resolved distance which is computed in this fashion is a probabilistic quantity. Thus, the predicted ground resolved distance is not equal to the actual ground resolved distance. Instead, the predicted ground resolved distance implies that the probability that the actual ground resolved distance is smaller than the predicted value is between 64 and 84 percent. Therefore, the average predicted ground resolved distance is larger than the average actual ground resolved distance.

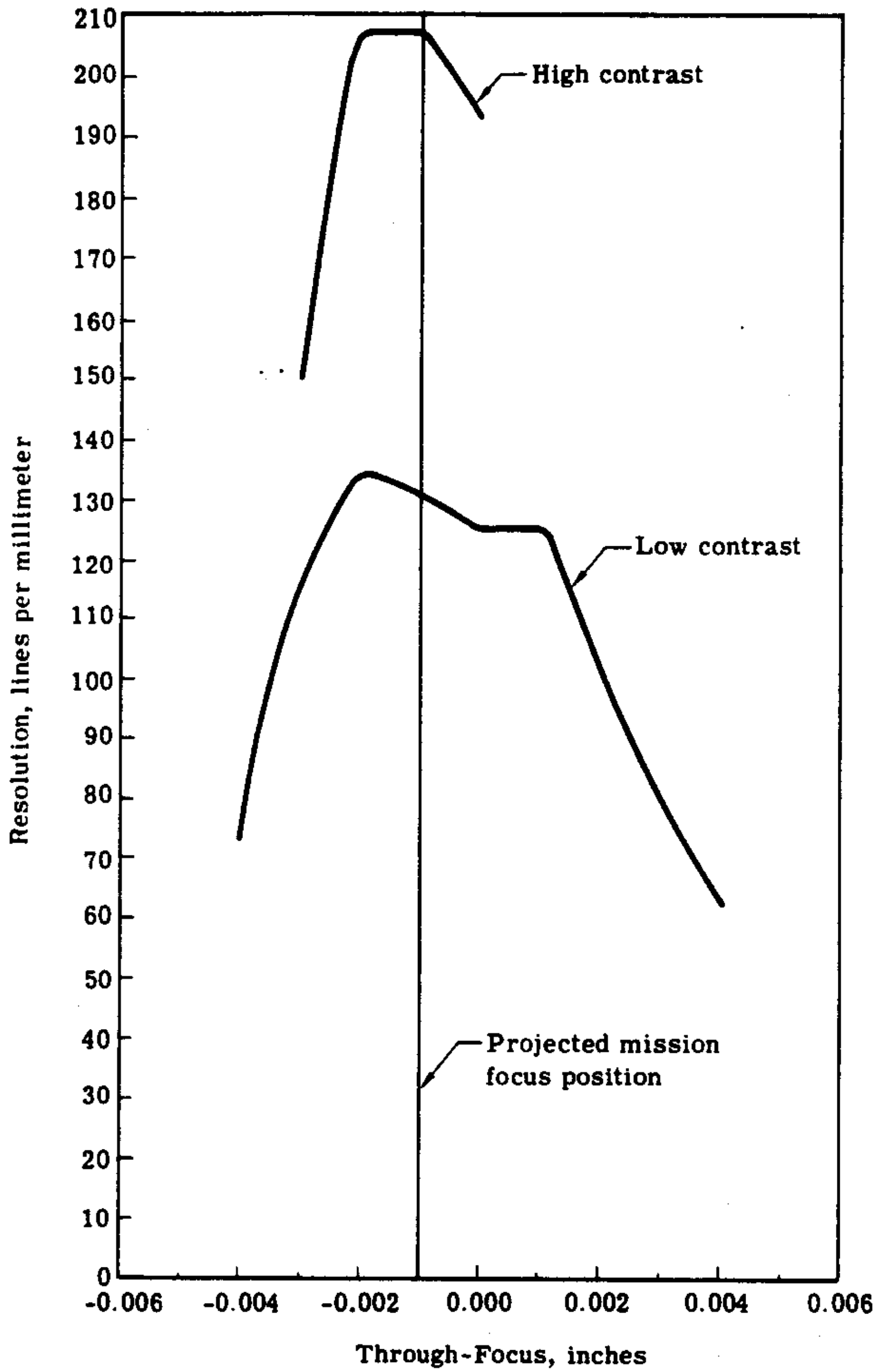


Fig. 3-1 — Dynamic resolution versus focus position (forward-looking camera, along track, unit no. 305)

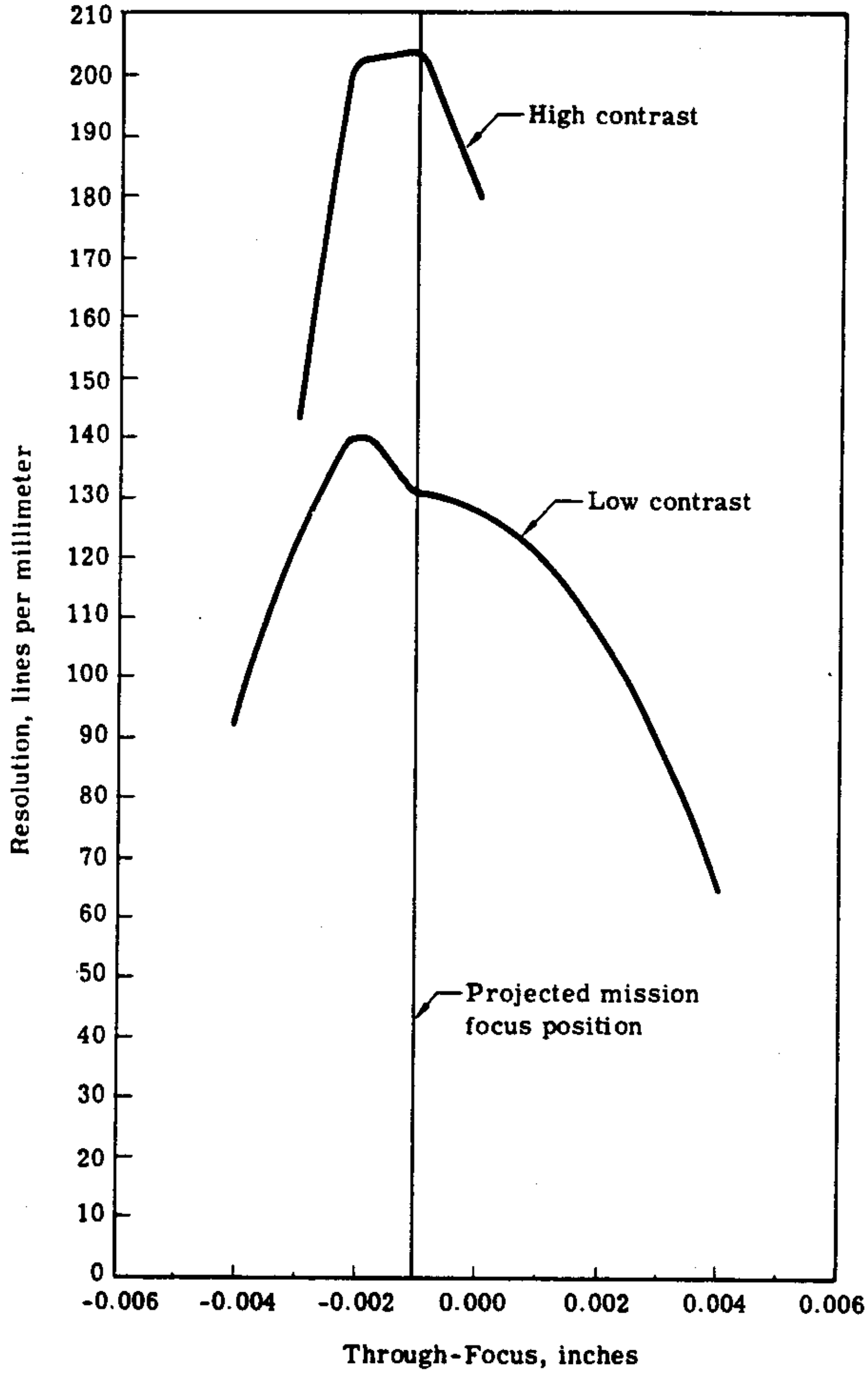


Fig. 3-2 — Dynamic resolution versus focus position (forward-looking camera, cross track, unit no. 305)

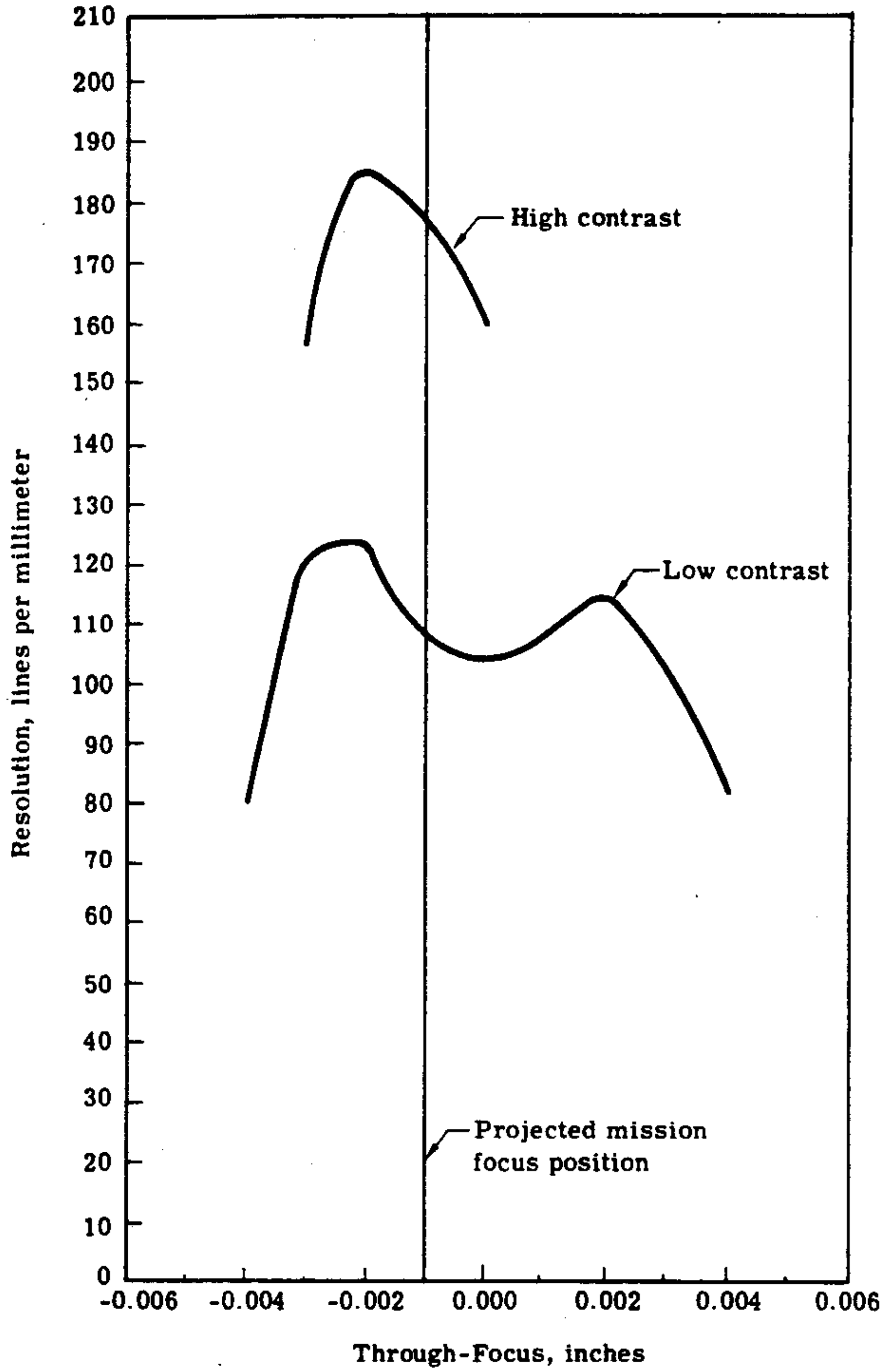


Fig. 3-3 — Dynamic resolution versus focus position (aft-looking camera, along track, unit no. 304)

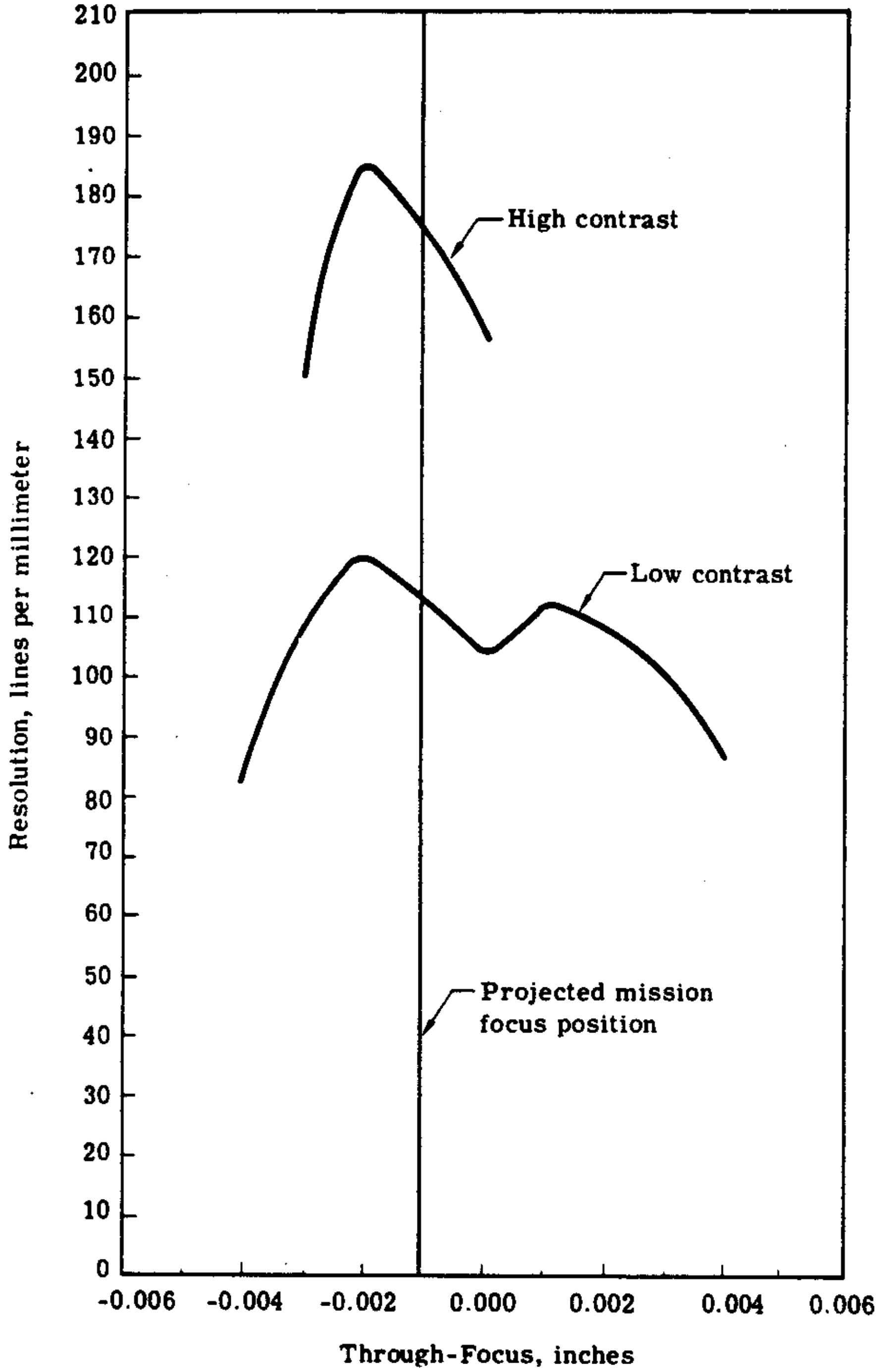


Fig. 3-4 — Dynamic resolution versus focus position (aft-looking camera, cross track, unit no. 304)

Resolution predictions were computed for the CORN targets of Table 3-1 and the HPL targets of Appendix A. For these targets, the SRV tape recorder summary was examined to determine if an abnormal number of jet firings took place which would indicate possible vehicle disturbances and unusually high vehicle rates. For all of the targets mentioned above, the jet firing activity appeared normal.

It was observed that the temperature inside the vehicle became colder (below 70°F) as the mission progressed. Table 3-4 shows the rail temperatures that were recorded. As the temperature of a panoramic camera is reduced, the effective film lift during the exposure of a frame is increased. In turn, film lift produces an image smear component in the cross-track direction which is directly proportional to the amount of film lift. A special test was performed with the purpose of determining the change in film lift as a function of temperature. The test results showed that, on the average, film lift increased at a rate of 0.0021 inch per 10°F in temperature drop. The corresponding increase in image smear was computed and factored into the resolution predictions in order to reflect the temperature environments shown in Table 3-4.

Table 3-4 — Rail Temperatures, °F

| Pass | Fwd-Looking Camera | Aft-Looking Camera | Pass | Fwd-Looking Camera | Aft-Looking Camera |
|---|---|---|---|---|---|
| 9 | 65 | 64 | 113 | 55 | 55 |
| 16 | 61 | 62 | 122 | 59 | 58 |
| 25 | 65 | 64 | 129 | 54 | 54 |
| 32 | 61 | 62 | 134 | 58 | 57 |
| 41 | 64 | 63 | 145 | 54 | 54 |
| 48 | 60 | 61 | 154 | 56 | 55 |
| 56 | 64 | 64 | 160 | 53 | 53 |
| 65 | 60 | 61 | 170 | 56 | 55 |
| 73 | 64 | 62 | 178 | 52 | 53 |
| 81 | 59 | 61 | 186 | 55 | 55 |
| 90 | 64 | 61 | 194 | 49 | 50 |
| 97 | 55 | 56 | 203 | 57 | 55 |
| 106 | 60 | 58 | 210 | 48 | 50 |

Several other laboratory tests were performed with the intention of determining the image motion at various points on the panoramic format. The targets utilized were crosshairs. Exposure was accomplished with a pair of narrow slits at the scan head of the panoramic camera under test. Thus, the panoramic frames produced contained doubly exposed images of the crosshair targets. If there was no image motion while a panoramic frame was being scanned, then the doubly exposed images of the same target would be superimposed on each other. Alternatively, if there was some image motion, the two images of the same target would be slightly displaced from each other on film. The spatial displacement of the two images is the image motion that occurred in the time interval between exposures. These tests were performed on unit no. 299 on ultrathin base film at the contractor's laboratory. The measurements of the image displacement were performed by the Data Analysis Center. Since these tests did not utilize 3404 film or one of the 1102 cameras, there is uncertainty as to whether they correctly represent the actual image motion conditions existing on the 1102 cameras. Hence, no attempt was made to utilize the results of these tests in the reported resolution predictions.

The vacuum and thermal tests that were performed on two Petzval lenses in the TORF chamber provided the following useful information:

1. The air-to-vacuum focus shift is approximately 0.014 to 0.0145 inch.

2. There is essentially no change in focus as a function of temperature as long as the temperature of the lens is uniform and there are no temperature gradients.

3. The focus shift is less than 0.0005 inch per 10°F temperature differential between the scan head and the rest of the lens.

4. In vacuum, if the front element of the lens faces a body of higher or lower temperature, a radial temperature gradient may develop between the center and the edges of the front element. The result of this temperature gradient is a shift in the lens focus as well as a degradation of lens performance.

Apparently, the temperature of the 1102 vehicle was not controlled completely, and it is possible that while the panoramic cameras were inoperative (lenses not rotating but stowed), one side of the vehicle was probably colder and the other side warmer than normal. Thus, one lens was probably facing a cold surface while its scan head was facing a warm surface. The reverse must have been true for the other lens because the lenses are stowed in opposite directions. It is then conceivable that one of the lenses experienced a focus shift in one direction while the other lens experienced a focus shift in the opposite direction. The temperature gradients of the Petzval lenses during the mission have been computed using a modified thermal model of the camera system. It appears that for the temperature gradients which were predicted, the focus shifts were not larger than 0.0003 inch.

### 3.3 COMPARISON OF CORN TARGET AND PREDICTED RESOLUTIONS

A fair comparison between a CORN target reading and the corresponding predicted ground resolved distance cannot be conducted without a knowledge of the apparent contrast of the target at the lens aperture. Resolution predictions have been computed for very high contrast and low contrast (2:1) tri-bar targets. On the ground, the contrast of the CORN targets is a nominal 4.7:1. The fixed targets are usually of higher contrast, about 10:1, but their real contrast at the lens apertures is unknown, and depends on how well the targets are maintained.

On the other hand, during the photographic mission, the contrast of all ground objects including resolution targets is reduced by the atmosphere. The loss in contrast is affected by weather conditions as well as solar elevation and azimuth. In Section 3.1 of the 1101 performance analysis report, the relationships between contrast and modulation are described. In the same section, a method for determining the apparent CORN target contrast at the lens aperture is also described. This method requires that microdensitometer traces be obtained on the original negative of the edge target which is part of the CORN target display. The fixed target displays have no edge targets. Thus, for the fixed targets, the apparent target contrast or modulation cannot be computed. Also, for unknown reasons, a number of CORN targets were not traced. Therefore, apparent contrast values have been computed for very few CORN targets. To compensate for the lack of this information, estimates of weather conditions and photographic contrast obtained by visually examining the panoramic and index camera records have been entered.

Tables 3-5 and 3-6 provide a means of comparing the CORN target readings with the predicted ground resolved distances. The columns identified as Average Reading have entries which are essentially the corresponding average readings taken from Table 3-2. The predicted ground resolved distances are low contrast (0.333 modulation) values. The modulation values entered in Tables 3-5 and 3-6 are the apparent target modulations which were computed from the available CORN target edge traces.

Examination of Tables 3-5 and 3-6 shows that 67 percent of the predicted ground resolved distances correlate very well with the average target readings.

## 3.4 EVALUATION OF SYSTEM OPERATION

While the other sections of this report attempt to establish the performance level of the 1102 system, this section is devoted to methods and techniques which could have improved and optimized the 1102 system's performance. This kind of evaluation will, hopefully, provide valuable information for the optimization of subsequent systems. For this evaluation, the system error budgets have been utilized as yardsticks. The error budgets have served as guidelines in the design and development of the panoramic camera system, and they indicate the performance capability of the 1100 series camera systems.

If the 1102 system performance is compared with the performance level predicted by the error budgets, the steps required to bring the 1102 system performance to the level anticipated by the error budgets become obvious. In addition, ways to surpass the performance level indicated by the error budgets are sought.

The flight data which have been analyzed and other laboratory data as well as the output of our computer program (see Appendix A) allowed a comparison of the 1102 system performance with the error budgets to be made. On the other hand, comparing the CORN target readings with the ground resolved distances predicted by the computer program has helped us to refine and improve the computer program.

For the CORN and HPL targets for which resolution predictions were computed, the average operating altitude turned out to be 87.6 nm. It should be obvious that the average ground resolved distance could be reduced almost 10 percent by operating at an average altitude of 80 nm. The panoramic cameras have been designed to operate at 80 nm, and if the vehicle could operate at this altitude, then the system performance can be improved by reducing the altitude.

The computer program showed that the systematic smear in the along-track direction was somewhat high. Therefore, the match between the V/h rates taken from the ephemeris and the camera FMC rates determined from the center-of-format switch closures were investigated. It was found that, on the average, both cameras were operating approximately 1.8 percent too fast. This in turn indicates that the V/h programmer was, on the average, producing voltages approximately 1.8 percent larger than those required. Equation (3.3) shows the FMC rate required for a given V/h rate:

$$\text{FMC} = \frac{V}{h} \cos^2 \phi - \dot{\beta} \tag{3.3}$$

where FMC = FMC rate

$\phi$ = camera half stereo angle (nominally, 15.23 degrees)

$\dot{\beta}$ = orbital pitching rate (nominally, $1.161 \times 10^{-3}$ radian per second for a 90-minute circular orbit)

V = actual orbital velocity of vehicle

h = vehicle altitude

Table 3-5 — CORN Target Readings and Predictions, feet (Fwd Camera)

| Pass | Frame | Along Track: Average Reading | Along Track: Modulation | Along Track: Predicted GRD | Cross Track: Average Reading | Cross Track: Modulation | Cross Track: Predicted GRD | Weather | Contrast | Target Type |
|---|---|---|---|---|---|---|---|---|---|---|
| 16 | 6 | 7.7 | – | 8.4 | 7.9 | – | 7.5 | Clear | Fair | Fixed, medium contrast |
| 32 | 13 | 8-12 | – | 7.8 | 8-12 | – | 7.00 | Clear | Fair | CORN |
| 48 | 21 | 8-12 | 0.061 | 7.7 | 12-16 | 0.061 | 6.4 | Cloudy | Low | CORN |
| 48 | 48 | 6.9 | – | 7.5 | 6.5 | – | 7.4 | Clear | Good | Fixed |
| 97 | 15 | 8-12 | – | 8.6 | 12-16 | – | 14.7 | Clear | Fair | CORN |
| 113 | 24 | 13.2* | – | 9.1 | 25* | – | 24.6 | Slight haze | Poor | Fixed |
| 176 | 26 | 11* | – | 7.3 | >16* | – | 6.4 | Heavy haze, cloudy | Poor | Fixed |

*Dupe positive readings only.

Table 3-6 — CORN Target Readings and Predictions, feet (Aft Camera)

| Pass | Frame | Along Track: Average Reading | Along Track: Modulation | Along Track: Predicted GRD | Cross Track: Average Reading | Cross Track: Modulation | Cross Track: Predicted GRD | Weather | Contrast | Target Type |
|---|---|---|---|---|---|---|---|---|---|---|
| 16 | 12 | 8.7 | – | 8.1 | 9.2 | – | 7.7 | Clear | Fair | Fixed, medium contrast |
| 32 | 19 | 8-12 | – | 8.0 | 10 | – | 7.3 | Clear | Fair | CORN |
| 48 | 54 | 8.1 | – | 8.2 | 7.2 | – | 8.4 | Clear | Good | Fixed |
| 97 | 21 | 13.3 | 0.239 | 9.1 | 12-16 | 0.239 | 11.9 | Clear | Fair | CORN |
| 176 | 32 | 10.5* | – | 8.0 | >16* | – | 8.0 | Cloudy, heavy haze | Poor | Fixed |

*Dupe positive readings only.

In turn, the camera scanning and FMC rates are related by Equation (3.4)

$$FMC = (CAM)(SCAN) \quad (3.4)$$

where CAM = camera cam constant (nominally, 0.01321)
SCAN = scanning rate

In addition, the FMC rate error for individual HPL targets varied from 0.10 to 3.9 percent. The allowable rms error in the error budgets for V/h control of the panoramic cameras is 1.41 percent.

The ephemeris data have been examined for clues to the apparent FMC rate errors. The scanning rates listed show a 0 to 3 percent variation in the scanning rates of successive frames. An examination of mission 1101 ephemeris showed a similar variation in the scanning rates.

On the other hand, the CORN target readings indicate that these scanning rate variations possibly are not real, but rather are errors in the data. The resolution predictions were computed on the assumption that the scanning rate information in the ephemeris is accurate. Thus, it is felt that one of the reasons for not achieving a much higher correlation between the CORN target readings and the predictions is that the 0 to 3 percent variation in the scanning rates between successive frames was possibly erroneous. It was later verified that in the computation of scanning rates, significant truncation errors were accidentally introduced by the computer, and these truncation errors accounted for most of the frame to frame variation of the scanning rates. In any case, it is recommended that a thorough investigation be made of the V/h programming of the 1100 series system. The average V/h error of 1.8 percent seems to be real and therefore all possible means should be utilized to eliminate this error.

A byproduct of the 1104 PG (panoramic geometry) calibration is the discovery of a resonant vibration frequency in the panoramic cameras which produces image smear in the along-track direction. In the PG calibration, the scan angle positions of the rail holes are determined accurately by utilizing a calibrated optical encoder mounted on the scanning shaft of the respective panoramic camera. Then, in order to determine the change of half-stereo angle (FMC angle) as a function of scan angle, several panoramic frames are obtained containing rail hole images and nod dots. The nod dots are generated by an accurate optical encoder mounted on the camera's nod shaft (FMC axis). Each nod dot is identified with a specific nod angle. The location of the nod dots among the rail hole images is determined by mensuration in a comparator. Thus, the change of nod angle over the panoramic format can be plotted as a function of scanning angle. Nominally, the nod angle should change linearly with scanning angle with a slope (cam constant) of 0.01321. During the 1104 PG calibration, several frames were reduced, and for each frame, a nod angle versus scanning angle function was plotted. These functions are fitted together in order to determine the cam constant. However, if each function is examined independently, it shows a small, approximately sinusoidal component superimposed on the linear variation of the nod angle. This sinusoidal component is present in all panoramic frames except that its phase in the various frames appears to be random. Thus, it seems that the unwanted sinusoidal variation of the cam constant is time-dependent and results from a natural vibration frequency of the panoramic cameras. The frequency of the sinusoidal variation was computed to be approximately 19.4 cps which agrees with the basic torsional frequency of the camera structure. The vibration causes a small sinusoidal variation to the camera cam constant, which in turn is reflected as a sinusoidal variation of the FMC rate. The result is a certain amount of image smear in the along-track direction.

From 1104 PG calibration data, it was determined that the rms image smear over the panoramic format is approximately 3 percent of the required FMC rate. The records of the 1102 PG calibration were examined and showed a similar variation in the camera cam constant. Thus, it appears that this effect is typical of the 1100 series panoramic cameras. In the error budgets, the allowable rms error in the cam constant is 1 percent. The camera performance would improve if the effects of camera vibration on the FMC rate could be reduced.

Ways by which the performance of the 1102 panoramic cameras could have been optimized will now be considered. All possibilities that were considered fall under one of the following general categories:

1. Reduction of image smear velocities
2. Reduction of exposure time
3. Reduction of altitude of photography
4. Improvement of lens focusing techniques
5. Optimization of lens-filter-exposure time combination.

In Table 3-7, various steps which would have improved the 1102 system performance with various degrees of success have been listed. In Table 3-8, the average expected ground resolved distances for the cases described in Table 3-7 have been entered. In Table 3-8 an attempt has been made to use identical values for all parameters which should be invariant between any two cases. This is essential in order to make a valid comparison. At the same time, data from mission 1102 have been used in order to make the comparison directly applicable to this mission. The data utilized was obtained by averaging the respective data from the CORN and HPL targets. Thus, average image smear, average static lens resolutions, and average scale factors were determined for the CORN and HPL targets.

Case B in Tables 3-7 and 3-8 is simply an interchange of the lenses of the panoramic cameras. A slight improvement in performance can be obtained by pairing the best lens of the system with the aft-looking camera where exposure times are shorter because of the W-21 filter.

Case C shows that a significant improvement in the ground resolved distance would have resulted if a W-21 filter was used in the forward-looking camera. Of course, some reduction in the contrast of the targets would have resulted in the forward-looking camera, but the gain in resolution would have more than offset the loss in contrast. The basic observation about the forward-looking camera is that its performance was image-smear limited in the cross-track direction, and that the image smear could have been reduced either by reducing the exposure time or by reducing the image smear velocities. In any case, the 0.340-inch slit should not have been used in the forward-looking camera. Instead, Case C shows that better results could have been obtained by reducing the slit size and utilizing a W-21 filter.

Case $E_{P.F.-80}$ shows the optimum performance level of which the 1102 system was capable. For this case, the following assumptions have been made:

1. Both lenses are optimally focused.
2. Both lenses carry W-21 filters.
3. The average altitude of photography is 80 nm.
4. The image smear velocities have been reduced to values which it is felt should be achievable.

Case $F_{P.F.-80}$ is similar to Case $E_{P.F.-80}$ except that all image smears have been assumed to be zero. This case is, of course, unrealistic, but it has been presented in Table 3-8 to show that image smear need not be eliminated entirely in order to achieve a system performance very close to the ultimate performance dictated by the quality of the lenses and film as well as altitude.

Comparing Cases $E_{P.F.-80}$ and A shows that there is plenty of room for improving the panoramic system performance. Case $E_{P.F.-80}$ represents a 36 percent improvement in performance over Case A.

Table 3-7 — List of System Configurations

| Case | Description |
|---|---|
| A | Actual mission 1102 configuration: aft-looking camera with a W-21 filter and lens I-165; forward-looking camera with a W-25 filter and lens I-181. |
| B | Aft-looking camera with lens I-181 and W-21 filter; forward-looking camera with lens I-165 and W-25 filter. |
| C | Aft-looking camera with lens I-165 and W-21 filter; forward-looking camera with lens I-181 and W-21 filter. |
| D | Image smear velocity reduced to about 1 millimeter per second; aft-looking camera with lens I-165 and W-21 filter; forward-looking camera with lens I-181 and W-25 filter. |
| E | Image smear velocity reduced to about 1 millimeter per second; aft-looking camera with lens I-165 and W-21 filter; forward-looking camera with lens I-181 and W-21 filter. |
| F | Theoretical (no image smear) performance; system configuration as in Case C. |
| $A_{80}$ through $F_{80}$ | Similar to respective Cases A through F except the mean altitude of photography is reduced from 87.6 to 80 nm. |
| $A_{P.F.}$ through $F_{P.F.}$ | Similar to respective Cases A through F except lenses operating at optimum focus. |
| $A_{P.F.-80}$ through $F_{P.F.-80}$ | Similar to respective Cases A through F except lenses operating at optimum focus and mean altitude of photography reduced to 80 nm. |

Table 3-8 — Comparative Chart of Average System Performance

| Case | Forward-Looking Camera: Along-Track Low Contrast GRD, feet | Forward-Looking Camera: Cross-Track Low Contrast GRD, feet | Aft-Looking Camera: Along-Track Low Contrast GRD, feet | Aft-Looking Camera: Cross-Track Low Contrast GRD, feet |
|---|---|---|---|---|
| A | 8.3 | 13.9 | 8.7 | 11.1 |
| B | 7.5 | 11.1 | 9.4 | 13.3 |
| C | 7.5 | 11.1 | 8.7 | 11.1 |
| D | 7.8 | 8.7 | 8.6 | 8.8 |
| E | 7.4 | 8.0 | 8.6 | 8.8 |
| F | 7.2 | 7.7 | 8.4 | 8.6 |
| $A_{80}$ | 7.6 | 12.7 | 8.0 | 10.2 |
| $B_{80}$ | 6.9 | 10.1 | 8.6 | 10.2 |
| $C_{80}$ | 6.9 | 10.1 | 8.0 | 10.2 |
| $D_{80}$ | 7.1 | 8.0 | 7.8 | 8.1 |
| $E_{80}$ | 6.8 | 7.3 | 7.8 | 8.1 |
| $F_{80}$ | 6.6 | 7.0 | 7.7 | 7.8 |
| $A_{P.F.}$ | 7.6 | 13.8 | 7.5 | 10.2 |
| $B_{P.F.}$ | 6.8 | 11.0 | 8.2 | 12.5 |
| $C_{P.F.}$ | 6.8 | 11.0 | 7.5 | 10.2 |
| $D_{P.F.}$ | 6.8 | 8.6 | 7.4 | 7.4 |
| $E_{P.F.}$ | 6.7 | 7.8 | 7.4 | 7.4 |
| $F_{P.F.}$ | 6.4 | 7.6 | 7.1 | 7.1 |
| $A_{P.F.-80}$ | 6.9 | 12.6 | 6.8 | 9.3 |
| $B_{P.F.-80}$ | 6.2 | 10.1 | 7.5 | 11.4 |
| $C_{P.F.-80}$ | 6.2 | 10.1 | 6.8 | 9.3 |
| $D_{P.F.-80}$ | 6.2 | 7.8 | 6.7 | 6.7 |
| Goal $E_{P.F.-80}$ | 6.1 | 7.2 | 6.7 | 6.7 |
| $F_{P.F.-80}$ | 5.9 | 6.9 | 6.5 | 6.5 |

# 4. "A" TAKEUP EXPERIMENT

## 4.1 GENERAL

The A takeup experiment was undertaken to quantitatively define the image quality of the emulsion batch of type 3404 film used in this mission.

The experiment consists of a comparison of the image quality on samples of type 3404 film in terms of its resolution (AIM curves), granularity (rms), and modulation transfer function. The image quality of the flight film is reported as a function of specific environmental condition. These conditions are classified as follows:

1. Control: Current process control for 3404 film (3404-277).
2. Preflight control: Refrigerated film of the same emulsion batch that was used in the KH-4B camera (3404-401).
3. A takeup: Film run through the camera prior to launch and removed from the recovery capsule prior to processing (3404-401).

Using a daylight plus W-23A filtered source, resolving power targets (for resolution), edges (for MTF), and flashed density patches (for granularity measurement) were exposed onto the film samples and the samples were then processed with the mission film.

On mission 1102-1, different emulsion batches of 3404 film were used in the forward and aft cameras, the forward camera having the faster film. The image evaluation for the A takeup experiment was conducted using the faster film. The processing conditions on each Trenton processor were adjusted to compensate for the speed differential, but the image evaluation exposures were processed on the Trenton adjusted for the aft camera load. This resulted in a speed shift of approximately 0.09 log E faster than would have been expected from the intended process. The image quality samples, therefore, received more development than the related camera record, and this should be taken into consideration when examining any dissimilarity between the 1101 and 1102 measurements. It is believed that most of the differences in these results as compared to that of mission 1101 (Performance Analysis for the 1101 System, control no. [redacted] are from this difference in the processing. However, a fair assessment of this cannot be made until this work has been performed on the first four 1100 missions.

## 4.2 FILM RESOLUTION AND AIM CURVE DERIVATION

Using replicated exposure series target readings, resolution was established at six contrast levels. An analysis of variance (ANOVA) test was also performed to compare the resolution determined from 1101 film samples with those of 1102. There is a significant difference between the control, preflight, and A takeup samples of CR-2. There is also a significant difference between the control, preflight, and A takeup samples of CR-1 and CR-2.

Strips for the six contrasts (consisting of three exposure series of 11 steps read from high to low density by three readers) were produced and read for control (3404-277), preflight control (3404-401), and A takeup samples (3404-402).

Three targets were read by three readers for each exposure level, giving nine group element readings. These readings were made for all 11 exposure levels giving a total number of 99 group element readings per contrast. The group element readings were then converted to log resolution values for further analysis.* The nine log resolution values for each of the 11 exposure levels were averaged to yield 11 average log resolution values as a function of exposure. Because film resolution is considered to be the maximum read from a strip at whatever exposure produces it, the highest log resolution value was chosen from the series as representative of the film resolution for that strip or contrast level.

Based on the estimated mean and the variance associated with the nine readings used to estimate the mean, 95 percent confidence limits were established about the true mean. The 95 percent confidence limits, found in log form and converted to linear values, establish limits within which the true film resolution could be expected to lie 95 percent of the time. Table 4-1 lists the results of this reduction.

AIM curves were drawn from the reduced data for control, preflight control, and A takeup conditions. Modulation was plotted against resolution to produce each AIM curve. Thus, the final product consists of the AIM curves shown in Figs. 4-1, 4-2, and 4-3. The AIM curves from 1101 are also shown to facilitate the comparison.

In order to compare the three film samples from CR-1 and CR-2, an analysis of variance was performed to determine whether or not there was a significant difference between the samples. The results are summarized in Table 4-2 with the judgments being made at the alpha equals 0.05 level of significance.

The experimental design consisted of a two-variable repeated-measurement experiment. The two variables were the films and the contrast levels. The repeated measurements were the nine readings for each strip that yielded the highest average resolution. The F-values were computed from the mean square for the film, with the contrast level and residual all being compared to the within-groups variance.

An examination of the results in Table 4-1 reveals the following conclusions. The significant difference between the control, preflight, and A takeup samples of CR-2 is attributed to the difference between the control and A takeup samples, not between the control and preflight or preflight and A takeup samples. This significant difference should not be considered as major since the control is a different emulsion batch, and is included as a means of evaluating the process rather than the quality of the flight film. The major comparison, preflight versus A takeup, is not significantly different. Consequently, the environmental effects subjected to the A takeup sample had no apparent effect on the resolution.

There is a significant difference between the CR-1 and CR-2 control, preflight, and A takeup film samples. This difference is also obvious when examining the AIM curves in Figs. 4-1, 4-2, and 4-3. Note that in each situation the resolution of the 3404 used in CR-2 is lower than CR-1. The difference between the control samples would indicate that a change has occurred at some stage in the process, and not as a result of the different environmental conditions.

*Since resolution is a geometric function (i.e., the difference between 100 and 200 lines per millimeter is similar to 10 and 20 lines per millimeter, whereas the change from 100 to 120 is not the same as 200 to 220) the analysis is handled in a geometric function.

Table 4-1 — Results of Data Reduction

| Filter | Identification | Target Contrast | Target Modulation | Average Resolution, lines per millimeter | 1-σ Range Low | 1-σ Range High |
|---|---|---|---|---|---|---|
| 78 + 23A | Control (3404-277) | 1.08:1 | 0.0384 | 31 | 28 | 34 |
| 78 + 23A | Control (3404-277) | 1.15:1 | 0.0698 | 109 | 100 | 120 |
| 78 + 23A | Control (3404-277) | 1.26:1 | 0.1150 | 129 | 120 | 140 |
| 78 + 23A | Control (3404-277) | 1.70:1 | 0.2592 | 202 | 194 | 210 |
| 78 + 23A | Control (3404-277) | 2.63:1 | 0.4490 | 320 | 296 | 345 |
| 78 + 23A | Control (3404-277) | 5.14:1 | 0.6743 | 378 | 378 | 378 |
| 78 + 23A | Preflight (3404-401) | 1.08:1 | 0.0384 | 28 | 20 | 38 |
| 78 + 23A | Preflight (3404-401) | 1.15:1 | 0.0698 | 94 | 83 | 105 |
| 78 + 23A | Preflight (3404-401) | 1.26:1 | 0.1150 | 139 | 125 | 155 |
| 78 + 23A | Preflight (3404-401) | 1.70:1 | 0.2592 | 207 | 194 | 220 |
| 78 + 23A | Preflight (3404-401) | 2.63:1 | 0.4490 | 308 | 286 | 331 |
| 78 + 23A | Preflight (3404-401) | 5.14:1 | 0.6743 | 359 | 340 | 379 |
| 78 + 23A | A takeup (3404-401) | 1.08:1 | 0.0384 | 26 | 22 | 31 |
| 78 + 23A | A takeup (3404-401) | 1.15:1 | 0.0698 | 97 | 93 | 102 |
| 78 + 23A | A takeup (3404-401) | 1.26:1 | 0.1150 | 143 | 127 | 161 |
| 78 + 23A | A takeup (3404-401) | 1.70:1 | 0.2592 | 180 | 173 | 187 |
| 78 + 23A | A takeup (3404-401) | 2.63:1 | 0.4490 | 257 | 241 | 276 |
| 78 + 23A | A takeup (3404-401) | 5.14:1 | 0.6743 | 359 | 345 | 373 |

Table 4-2 — Difference Significance of Samples

| Comparisons | Difference Significant | Difference Not Significant |
|---|---|---|
| Control and preflignt and A takeup (CR-2) | * | |
| Control and preflight (CR-2) | | * |
| Control and A takeup (CR-2) | * | |
| Preflight and A takeup (CR-2) | | * |
| Control (CR-1) and control (CR-2) | * | |
| Preflight (CR-1) and preflight (CR-2) | * | |
| A takeup (CR-1) and A takeup (CR-2) | * | |

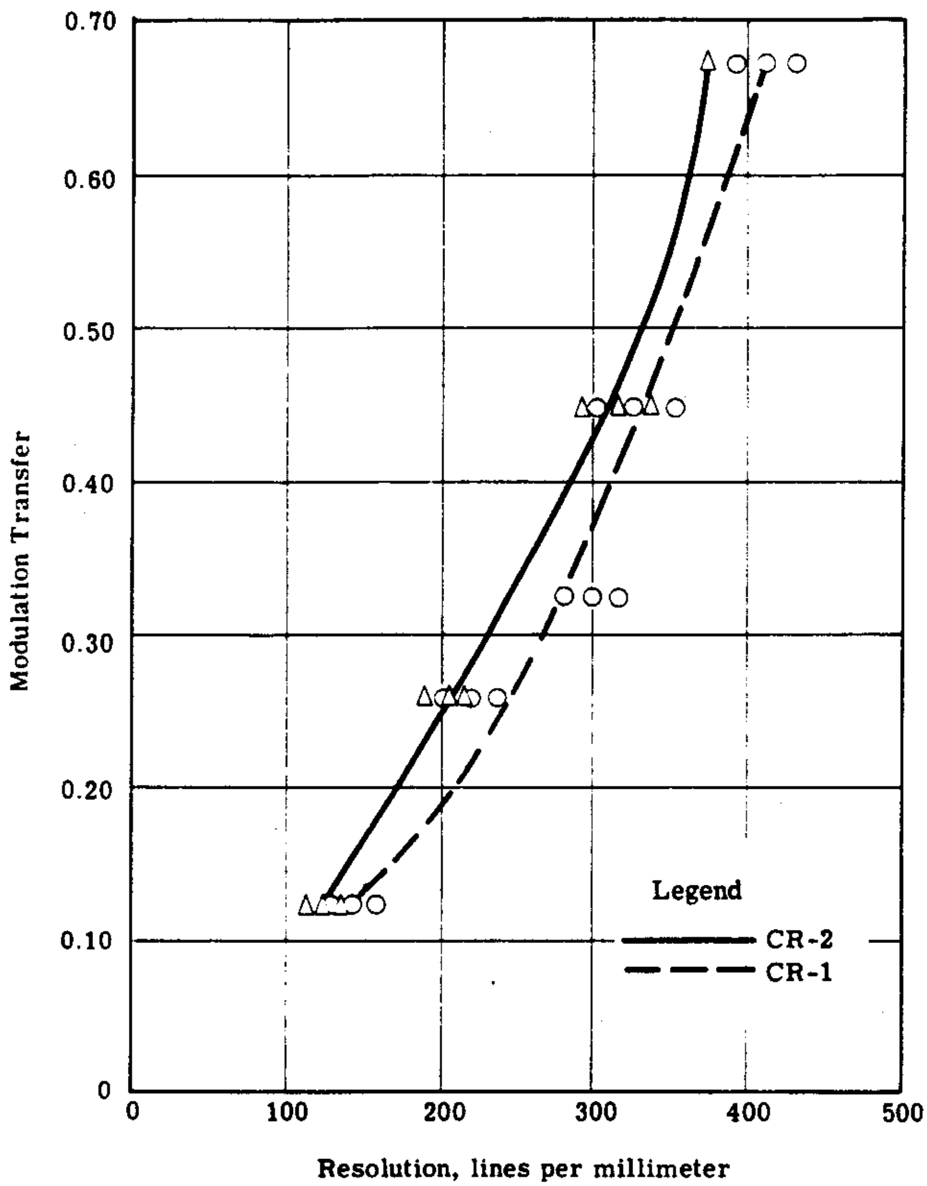


Fig. 4-1 — Test object modulation versus resolution (AIM) of the control film samples for CR-1 and CR-2

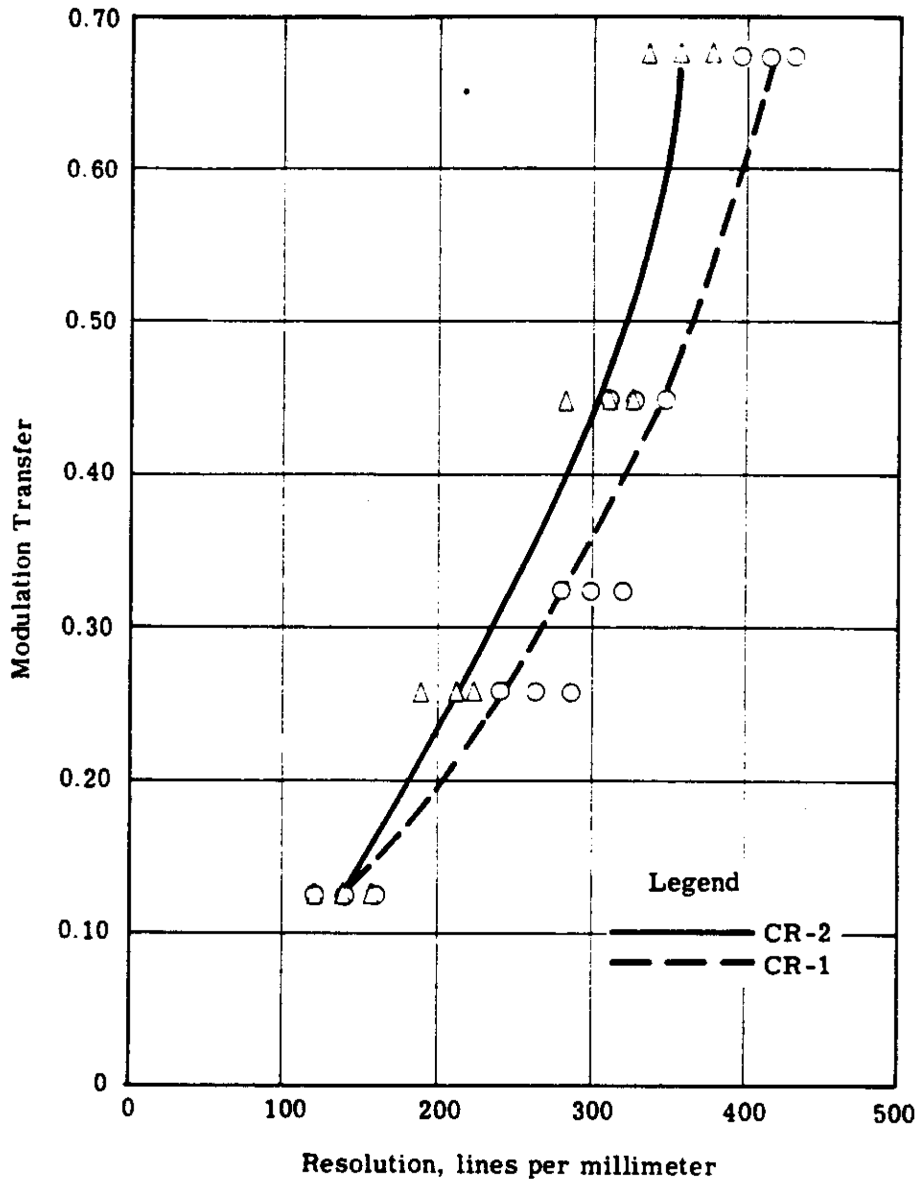


Fig. 4-2 — Test object modulation versus resolution (AIM) of the preflight control film samples for CR-1 and CR-2

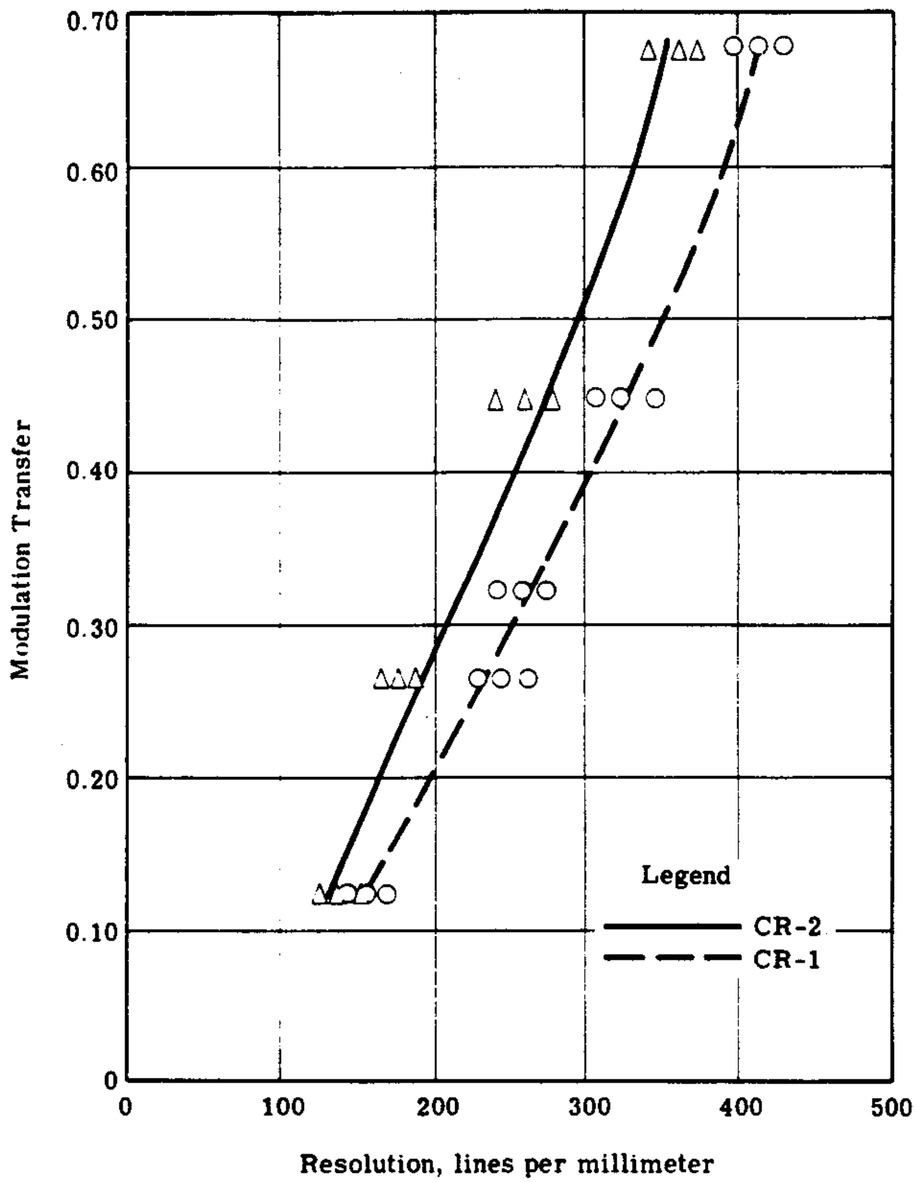


Fig. 4-3 — Test object modulation versus resolution (AIM) of the A takeup film samples for CR-1 and CR-2

## 4.3 RMS GRANULARITY

The rms granularity values were determined at four density levels for the control, preflight, and A takeup film samples. The resultant curves (granularity as a function of density) are shown in Fig. 4-4 and the granularity values at the 1.0 gross density granularity are included for purposes of comparison (Table 4-3).

The aperture size, 12 microns, was chosen as a result of discussion and agreement between Itek and Eastman Kodak personnel, as it was considered to be more in keeping with the viewing magnification to be used on the system product. To convert reported rms values thus determined to figures comparable to those obtained with a 24-micron aperture size, divide the values by 2 in conformance with Selwyn's Law.*

| | |
|---|---|
| Aperture size | 12 ± 1 micron |
| Data point spacing | Approximately 10 percent diameter overlap |
| Number of density patches per strip | 4 |
| Number of scans per density patch | 5 |
| Number of data points per scan | 500 |

The rms granularity values were computed for each of 60 scans using bad data elimination and detrending techniques. A pooled estimate of the variance and rms value was calculated for each patch.

The determination of whether or not a significant difference exists in the granularity within or between missions can be based on either of two criteria: statistical or psychophysical. The statistical criterion is easily implemented since it is based on the RMS variances applied in an F-test. This technique, however, takes into account only the variability inherent in the measured value. This test indicates that the values are indeed different. Although significant differences can be determined by statistics, it is questionable as to whether any confidence can be attached to them.

It is not known at this point how much of a difference in granularity is meaningful to the observer. The film samples themselves, though, do not look different under a high magnification.

## 4.4 FILM MODULATION TRANSFER FUNCTION

The modulation transfer function (MTF) of type 3404 film for the control, preflight, and A takeup samples of CR-2 were computed and are shown in Fig. 4-5(a); also included are the MTF's from CR-1. Examination of the MTF's from CR-2 indicate that there is no significant difference between the CR-1 and CR-2 control, preflight, and A takeup samples, with the CR-2 lower.

*Selwyn's Law states that granularity varies inversely proportional to the square root of the scanning aperture.

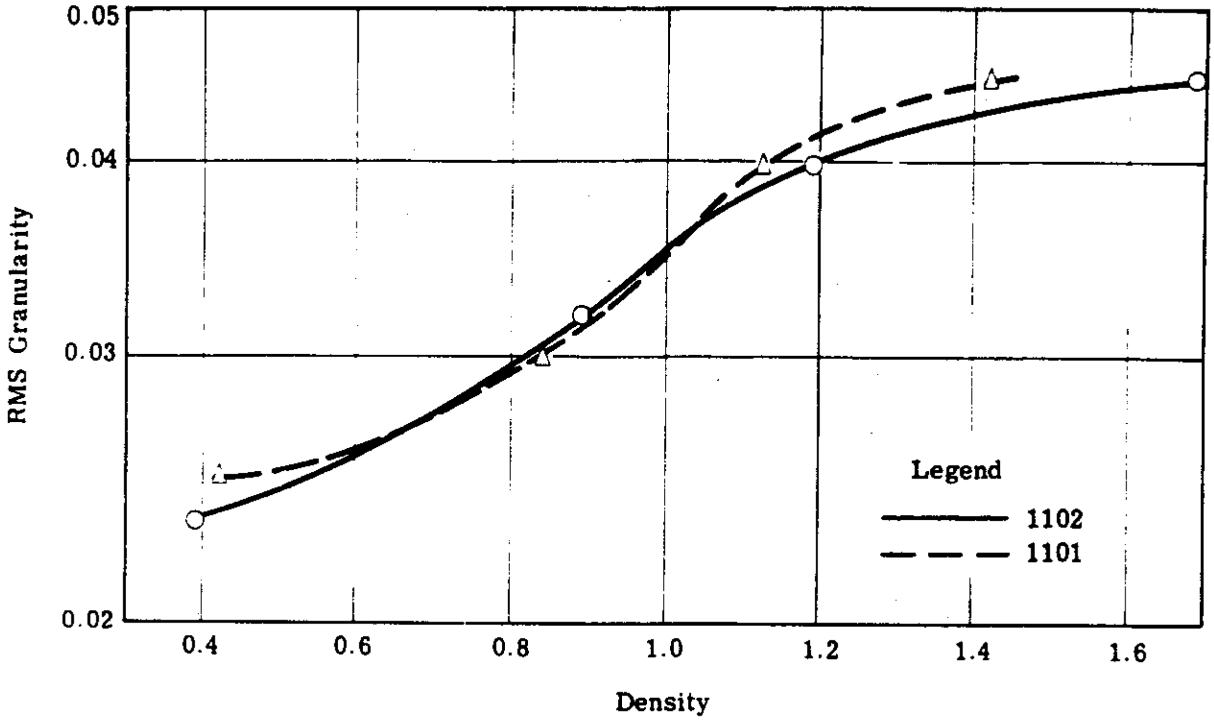


(a) Control

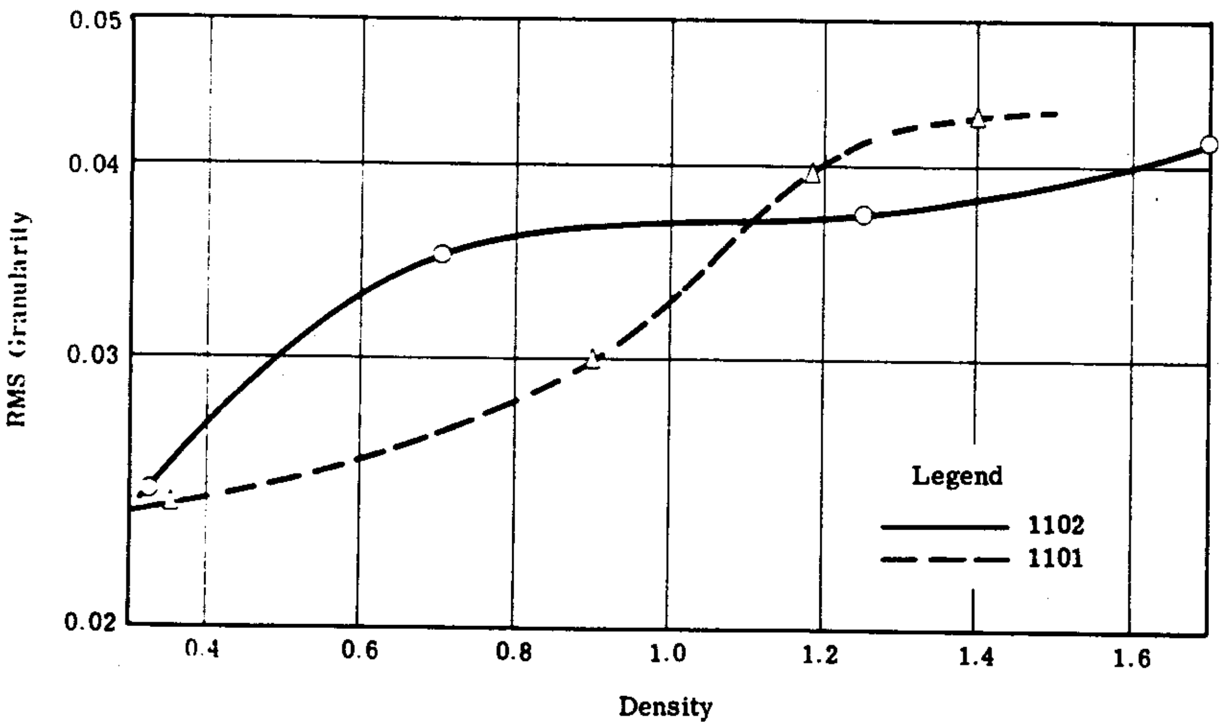


(b) Preflight

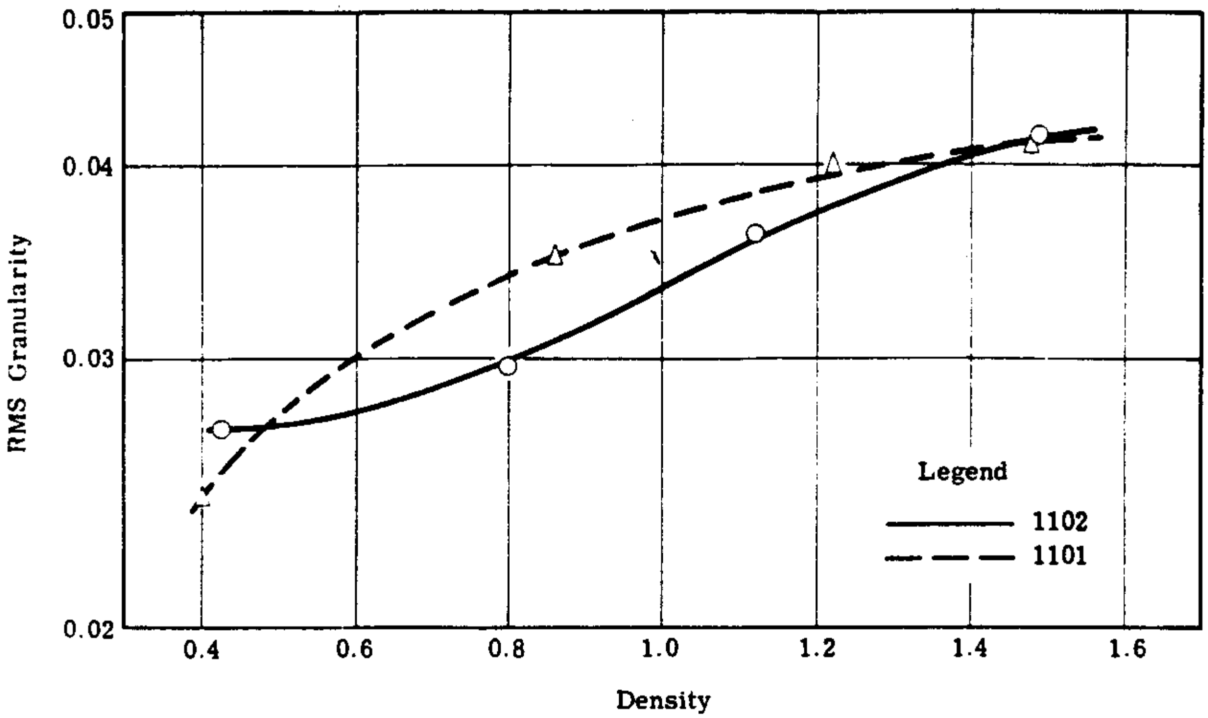


(c) A takeup

Fig. 4-4 — Granularity of film samples as a function of density for the 1101 and 1102 experiments

Table 4-3 — RMS Granularity at 1.0 Gross Density

| Condition | 1101 | 1102 |
|---|---|---|
| Control | 0.036 | 0.035 |
| Preflight | 0.034 | 0.037 |
| A takeup | 0.038 | 0.033 |

The modulation transfer functions were calculated in the following manner. High acquity edges of 2:1 and 4:1 contrasts were exposed onto the three film samples in the Eastman Kodak Microscope Camera. The samples were then processed along with the flight material. The 2:1 contrast edge was traced on the Itek Intectron Microdensitometer, with the resultant edge trace having a density range from approximately 0.4 to 1.7. The MTF for each of the three conditions is an average of five individually calculated functions. The MTF for the microdensitometer was removed so that the resultant MTF's are the best estimate of the film alone. Confidence limits of 95 percent were determined based on deviation of the five MTF's as shown in Figs. 4-5(a) and 4-5(b).

The difference between the MTF's of CR-1 and CR-2 are obvious since the confidence limits from the CR-1 data are high than those of CR-2 at almost all frequencies. This difference is a reflection of the resolution (AIM curve) conclusions, which verifies that the image quality measurements of the mission 1102 film has detected a significant change from the image quality of the mission 1101 film. However, it is assumed at this point that this is due to the processing conditions used.

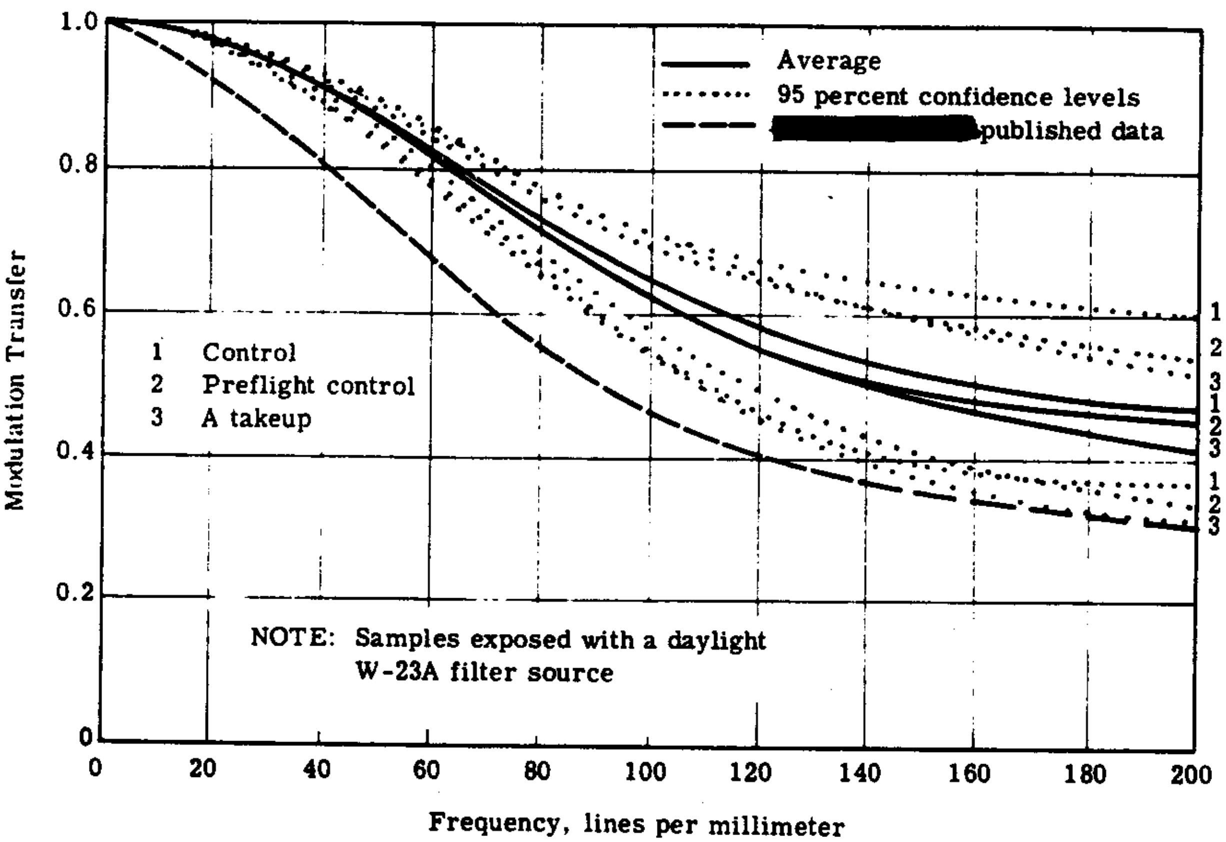


(a) Mission 1101

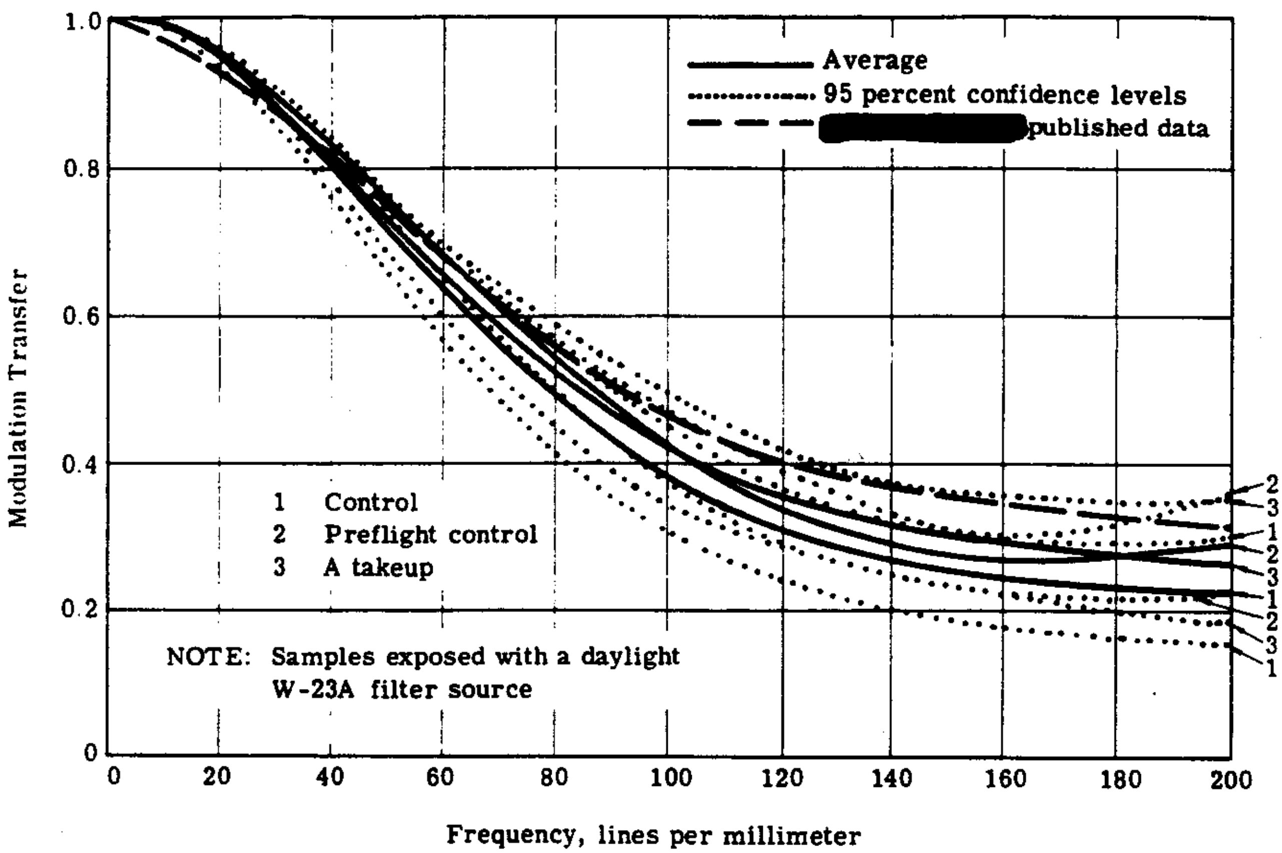


(b) Mission 1102

Fig. 4-5 — MTF of type 3404 film from A takeup experiment

# 5. DENSITY ANALYSIS

## 5.1 OBJECTIVE

The objective of the density analysis is to determine if the HPL targets on the 1102 mission were properly exposed.* The [redacted] terrain measurement technique is presently the method used to make the exposure judgments of the mission as a whole; however, investigation reveals that a serious drawback is associated with the use of this criterion. HPL edge tracing, however, gives an evaluation of the exposure to the areas of interest.

The HPL targets, which are of strategic importance located primarily in the Soviet Union and China, are scanned from the flight film original negative with a microdensitometer. The minimum and maximum densities of these traces are subjectively evaluated in terms of their location on the D-log E curve of the mission emulsion. The target minimum and maximum densities are then compared with the [redacted] terrain density measurements to ascertain whether a correlation exists between the two units and if one technique is more representative of the actual exposure conditions.

## 5.2 PROCEDURE

A single microdensitometer scan was made across the HPL targets. The scanning aperture was 10 microns in diameter, representing 8 to 10 feet on the ground. The traced area was chosen to cover the portions of the target which are of greatest interest to the photointerpreter. The traces were subjectively analyzed to determine the minimum and maximum densities. These densities and their corresponding pass, frame, camera, target number, slit, and filter are shown in Table 5-1.

The criterion for judging the exposure quality of a target is based on the film's characteristic curve. The minimum density should fall in an area of the curve where small exposure differences will be recorded as significant density differences. The maximum density should follow the same criterion, but at the same time not be so high an exposure as to produce a degradation in the image quality. For 3404 film, it has been decided that a minimum density below 0.4 is an underexposed condition; and a minimum density above 0.8, or a maximum density above 2.0, is an overexposed condition. A value of 0.8 has been chosen as an upper limit, since, with its particular curve shape for type 3404, it would require a full stop less exposure to bring it down to the 0.4 level.

The terrain densities, as determined by [redacted] are shown in Table 5-2. The terrain measurements were made with a densitometer having a 0.5-millimeter spot aperture. The number of measured frames was statistically determined so that a valid judgment could be made concerning the total mission. The mission was divided into four portions (the first and second buckets

---

*An error in terminology exists in the 1101 performance analysis report in the density analysis section. COMIREX Priority I targets were not necessarily the targets on the HPL that were measured.

Table 5-1 — Density Analysis of Mission 1102

| Pass | Frame | Camera | Target* | Slit | Filter | $D_{min}$ | $D_{max}$ |
|---|---|---|---|---|---|---|---|
| D-024 | 21 | F | 121 | 0.340 | W-25 | 0.94† | 1.84 |
| D-024 | 27 | A | 121 | 0.270 | W-21 | 0.76 | 1.65 |
| D-024 | 59 | F | 104 | 0.340 | W-25 | 0.43 | 1.07 |
| D-024 | 65 | A | 104 | 0.270 | W-21 | 0.69 | 1.64 |
| D-154 | 34 | F | 301 | 0.340 | W-25 | 1.01† | 1.77 |
| D-154 | 40 | A | 301 | 0.215 | SF-05 | 0.88† | 1.38 |
| D-007 | 20 | F | 120 | 0.340 | W-25 | 0.40 | 0.81 |
| D-007 | 26 | A | 120 | 0.270 | W-21 | 0.55 | 0.98 |
| D-120 | 28 | F | 120 | 0.340 | W-25 | 0.99† | 2.08 |
| D-120 | 34 | A | 120 | 0.270 | W-21 | 1.10† | 2.16 |
| D-021 | 60 | F | 106 | 0.340 | W-25 | 0.57 | 1.52 |
| D-021 | 66 | A | 106 | 0.270 | W-21 | 0.69 | 1.91 |
| D-039 | 48 | F | 31 | 0.340 | W-25 | 0.98‡ | 1.83 |
| D 039 | 54 | A | 31 | 0.270 | W-21 | 1.34‡ | 1.98 |
| D-072 | 6 | F | 302 | 0.340 | W-25 | 0.43 | 0.68 |
| D-072 | 12 | A | 302 | 0.270 | W-21 | 0.71 | 1.26 |
| D-087 | 8 | F | 303 | 0.340 | W-25 | 1.21† | 2.12 |
| D-087 | 14 | A | 303 | 0.270 | W-21 | 1.05 | 2.07 |
| D-089 | 2 | F | 105 | 0.340 | W-25 | 0.59 | 1.30 |
| D-089 | 8 | A | 105 | 0.270 | W-21 | 0.63 | 1.36 |
| D-186 | 3 | F | 105 | 0.215 | W-25 | 0.39§ | 1.18 |
| D-186 | 10 | A | 105 | 0.134 | W-21 | 0.33§ | 0.93 |
| D-120 | 6 | F | 122 | 0.340 | W-25 | 1.11† | 1.56 |
| D-120 | 12 | A | 122 | 0.270 | W-21 | 1.16† | 1.62 |
| D-137 | 10 | F | 103 | 0.340 | W-25 | 0.50 | 0.96 |
| D-137 | 16 | A | 103 | 0.270 | W-21 | 0.54 | 1.08 |
| D-167 | 4 | F | 80 | 0.340 | W-25 | 0.38‡ | 1.44 |
| D-167 | 10 | A | 80 | 0.170 | W-21 | 0.48 | 1.46 |

*Arbitrary number assigned for the purpose of this study by NPIC.
†Overexposure due to snow covered landscape.
‡No explanation.
§ Underexposure due to surrounding wooded area.

of the forward and aft cameras), and the total average minimum and maximum densities for each section are reported in Table 5-2.

Table 5-2 — [redacted] Average Terrain Densities

| Mission Portion | $D_{min}$ | $D_{max}$ |
|---|---|---|
| Fwd-1 | 0.50 | 1.23 |
| Aft-1 | 0.55 | 1.28 |
| Fwd-2 | 0.46 | 1.23 |
| Aft-2 | 0.47 | 1.30 |

5.3 RESULTS

An examination of the minimum and maximum densities in Table 5-1 indicates that of the 28 targets traced, 3 (or 11 percent) were underexposed, 11 (or 40 percent) were overexposed, for a total of 14 (or 51 percent) being incorrectly exposed. Both portions of passes D-154, D-139, D-087, and D-120, and one portion of pass D-024, were overexposed, and both portions of pass D-186 and one portion of pass D-167 were underexposed.

These underexposed and overexposed conditions can generally be explained by examining the particular target type, surrounding area, or exposure condition associated with each target. In most instances, the snow covered landscape caused the very high densities associated with an overexposed condition. In contrast, the wooded area surrounding the target on pass D-186 resulted in a low density and underexposure judgment.

There are two situations concerning the repeated coverage of a single target on two different passes which deserves an explanation. Target number 121 was covered on pass D-007 and D-120; however, it was judged to be overexposed only on the latter pass. Examination of the target revealed that during the time differential between the two passes it had snowed, which resulted in the overexposure condition. Target number 105 was covered on passes D-089 and D-186. The exposure time was reduced on the latter pass by approximately 1/4 stop, causing the target to be converted from an acceptable to an underexposed situation.

A comparison of the minimum densities from the HPL targets and the corresponding average minimum terrain densities from the four portions of mission 1102 are shown in Table 5-3. It is significant to note that of the 28 comparisons, the terrain densities are higher six times (or 22 percent of the total), the target densities are higher 21 times (or 75 percent of the total), and in one case they are equal. The number of higher target minimum densities surpass the number of higher terrain minimum densities. This might indicate that the frequency of underexposed judgments would be greater if the terrain rather than the target density technique were utilized.

## 5.4 CONCLUSIONS

The exposure quality of the targets in mission 1102 (based on the HPL target densities) was generally overexposed. Eleven (or 40 percent) of targets were overexposed and only three (or 11 percent) were underexposed.

A majority of the overexposed conditions are a result of snow cover at the target area. Both portions of pass D-039 were overexposed and one portion of pass D-167 was underexposed and there appears to be no obvious reason for these conditions.

Table 5-3 — Terrain Versus Target $D_{mins}$

| Target | Terrain | Target | Terrain |
|---|---|---|---|
| 0.94 | 0.50 | 1.21 | 0.46 |
| 0.76 | 0.55 | 1.05 | 0.47 |
| 0.43 | 0.50 | 0.59 | 0.46 |
| 0.69 | 0.55 | 0.63 | 0.47 |
| 1.01 | 0.46 | 1.11 | 0.46 |
| 0.88 | 0.47 | 1.16 | 0.47 |
| 0.40 | 0.50 | 0.99 | 0.46 |
| 0.55 | 0.55 | 1.10 | 0.47 |
| 0.57 | 0.50 | 0.50 | 0.46 |
| 0.69 | 0.55 | 0.54 | 0.47 |
| 0.98 | 0.50 | 0.38 | 0.46 |
| 1.34 | 0.55 | 0.48 | 0.47 |
| 0.43 | 0.50 | 0.39 | 0.46 |
| 0.71 | 0.55 | 0.33 | 0.47 |

Total of 28 Density Measurements

| | No. | Percent |
|---|---|---|
| Terrain higher | 6 | 22 |
| Target higher | 21 | 75 |
| Equal | 1 | 3 |

## 6. RECOMMENDATIONS

The following recommendations are offered concerning future missions of the 1100 series paroramic systems.

1. It is necessary to optimize the lens-film-filter-exposure time combinations for each mission. The filter that might be used directly affects the lens performance and the apparent target contrast at the lens aperture. In addition, it has an indirect effect on image smear by controlling the exposure times required. The optimum filter should be selected so that its effects on target contrast, lens performance, and image smear are balanced. It is conceivable that the optimum film-filter combinations of the panoramic cameras would vary with the time of the year of a mission. Also, changes in the panoramic cameras (i.e., reduction of the image smear velocities) would alter the optimum film-filter combinations.

2. Exposure times longer than 4 milliseconds should be avoided because the resulting image smears in either the along- or the cross-track direction become excessive.

3. The Petzval lenses should be dynamically focused in vacuum.

4. The average altitude of photography should be reduced to 80 nm.

5. The V/h programming errors should be corrected and the residual rms error should not exceed 1.5 percent of the required V/h rates. Also, a complete investigation concerning the V/h programmer and the scanning rate data of the SRV tape recorder should be undertaken. (See Section 3.4 for details.)

6. The along-track image smear due to camera vibration should be reduced so that the rms effect of camera vibration on the FMC rates should be less than 1.5 percent of the required FMC rate.

7. The image smear in the cross-track direction consists of the uncompensated image motion component and the film motion component resulting from the scanning motion of the scan head past the film. On the basis of the information presently available, it seems possible to introduce adjustments to the panoramic cameras which will tend to reduce significantly the cross-track image smear. Therefore, an investigation of this possibility should be conducted.

## Appendix A

## RESOLUTION PREDICTIONS FOR CORN TARGETS

This appendix is a listing of the image smear and resolution data which have been computed for the CORN targets (see Tables A-1 and A-2).

### Notation

| | | |
|---|---|---|
| BALTR | = | image smear, along track, random, microns |
| BALTS | = | image smear, along track, systematic, microns |
| TBAT | = | total blur, along track, microns |
| RESL | = | dynamic film resolution, along track, low contrast (2:1), lines per millimeter |
| RESH | = | dynamic film resolution, along track, high contrast, lines per millimeter |
| GDRL | = | ground resolution, along track, low contrast, feet |
| GDRH | = | ground resolution, along track, high contrast, feet |
| BCTR | = | image smear, cross track, random, microns |
| BCTS | = | image smear, cross track, systematic, microns |
| TBCT | = | total image smear, cross track, microns |
| CRESL | = | dynamic film resolution, cross track, low contrast, lines per millimeter |
| CRESH | = | dynamic film resolution, cross track, high contrast, lines per millimeter |
| CGDRL | = | ground resolution, cross track, low contrast, feet |
| CGDRH | = | ground resolution, cross track, high contrast, feet |

Table A-1 — Resolution Predictions for CORN Targets, Forward-Looking Camera, Unit No. 305

| Pass | 16 | 32 | 48 | 48 | 97 | 113 | 176 |
|---|---|---|---|---|---|---|---|
| Frame | 6 | 13 | 21 | 48 | 15 | 24 | 26 |
| **Along Track** | | | | | | | |
| BALTR | 3.24 | 2.81 | 3.40 | 3.37 | 3.25 | 2.91 | 3.36 |
| BALTS | 2.19 | -1.95 | -1.51 | -0.32 | 3.18 | 2.63 | 0.31 |
| TBAT | 5.43 | 4.76 | 4.90 | 3.69 | 6.43 | 5.54 | 3.66 |
| RESL | 116.0 | 119.5 | 121.0 | 126.7 | 112.0 | 117.8 | 126.0 |
| RESH | 157.5 | 168.1 | 166.4 | 187.7 | 138.4 | 153.6 | 189.4 |
| GDRL | 3.4 | 7.8 | 7.7 | 7.5 | 8.6 | 9.1 | 7.3 |
| GDRH | 6.2 | 5.5 | 5.6 | 5.1 | 6.9 | 7.0 | 4.8 |
| **Cross Track** | | | | | | | |
| BCTR | 0.96 | 0.85 | 1.01 | 1.00 | 0.96 | 0.82 | 1.00 |
| BCTS | -3.66 | 3.56 | -1.55 | -3.27 | 13.50 | 18.64 | -1.83 |
| TBCT | 4.61 | 4.41 | 2.56 | 4.27 | 14.46 | 19.46 | 2.82 |
| CRESL | 131.9 | 128.1 | 143.2 | 128.1 | 65.4 | 49.6 | 143.2 |
| CRESH | 178.7 | 175.7 | 220.1 | 177.1 | 67.2 | 50.0 | 207.8 |
| CGDRL | 7.5 | 7.0 | 6.4 | 7.4 | 14.7 | 24.6 | 6.4 |
| CGDRH | 5.5 | 5.1 | 4.2 | 5.3 | 14.3 | 24.4 | 4.4 |

Table A-2 — Resolution Predictions for CORN Targets, Aft-Looking Camera, Unit No. 304

| Pass | 16 | 32 | 48 | 97 | 176 |
|---|---|---|---|---|---|
| Frame | 12 | 19 | 54 | 21 | 32 |
| **Along Track** | | | | | |
| BALTR | 2.57 | 2.82 | 2.59 | 2.49 | 1.62 |
| BALTS | 1.99 | -2.62 | 1.10 | 2.41 | 1.25 |
| TBAT | 4.56 | 5.44 | 3.68 | 4.90 | 2.87 |
| RESL | 121.8 | 116.5 | 114.2 | 102.3 | 114.1 |
| RESH | 157.4 | 145.5 | 161.8 | 144.6 | 167.4 |
| GDRL | 8.1 | 8.0 | 8.2 | 9.1 | 8.0 |
| GDRH | 6.3 | 6.4 | 5.8 | 6.4 | 5.4 |
| **Cross Track** | | | | | |
| BCTR | 0.76 | 0.85 | 0.77 | 0.73 | 0.48 |
| BCTS | -2.93 | 3.82 | -2.18 | 10.61 | -0.61 |
| TBCT | 3.69 | 4.67 | 2.94 | 11.35 | 1.10 |
| CRESL | 129.7 | 122.7 | 112.1 | 79.8 | 113.9 |
| CRESH | 167.5 | 156.0 | 172.8 | 84.9 | 179.6 |
| CGDRL | 7.7 | 7.3 | 8.4 | 11.9 | 8.0 |
| CGDRH | 5.9 | 5.7 | 5.4 | 11.2 | 5.1 |

## Appendix B

## RESOLUTION PREDICTIONS FOR HPL TARGETS

Resolution predictions for HPL targets are contained in Tables B-1 and B-2. Table B-3 contains data concerning average low contrast ground resolution versus photointerpreter rating.

Table B-1 — Resolution Predictions for HPL Targets,
Forward-Looking Camera, Unit No. 305

| Target | 121 | 104 | 301 | 120 | 106 | 31 | 302 |
|---|---|---|---|---|---|---|---|
| Pass | 24 | 24 | 154 | 7 | 21 | 39 | 72 |
| Frame | 21 | 59 | 34 | 20 | 60 | 48 | 6 |
| **Along Track** | | | | | | | |
| BALTR | 3.23 | 3.13 | 3.01 | 3.26 | 3.29 | 3.25 | 3.19 |
| BALTS | 0.86 | 1.79 | 0.24 | 0.32 | 2.25 | 2.53 | 4.08 |
| TBAT | 4.09 | 4.93 | 3.25 | 3.58 | 5.54 | 5.78 | 7.27 |
| RESL | 122.6 | 122.3 | 131.8 | 128.0 | 117.9 | 113.9 | 106.9 |
| RESH | 181.9 | 164.7 | 197.3 | 190.9 | 153.4 | 149.1 | 125.8 |
| GDRL | 8.6 | 8.8 | 7.8 | 8.1 | 8.9 | 8.6 | 9.5 |
| GDRH | 5.8 | 6.6 | 5.2 | 5.4 | 6.8 | 6.6 | 8.1 |
| **Cross Track** | | | | | | | |
| BCTR | 0.95 | 0.90 | 0.86 | 0.96 | 0.97 | 0.96 | 0.94 |
| BCTS | -5.46 | 16.41 | 18.09 | 13.17 | 12.95 | 12.93 | 14.10 |
| TBCT | 6.41 | 17.31 | 18.95 | 14.13 | 13.92 | 13.89 | 15.04 |
| CRESL | 115.6 | 55.7 | 51.1 | 67.3 | 67.7 | 67.8 | 63.3 |
| CRESH | 140.1 | 56.2 | 51.4 | 68.8 | 69.7 | 69.8 | 64.6 |
| CGDRL | 9.3 | 20.6 | 22.2 | 15.6 | 15.5 | 14.5 | 16.4 |
| CGDRH | 7.7 | 20.4 | 22.1 | 15.3 | 15.1 | 14.1 | 16.0 |

Table B-1 — Resolution Predictions for HPL Targets,
Forward-Looking Camera, Unit No. 305 (Cont.)

| Target | 303 | 105 | 122 | 120 | 103 | 80 | 105 |
|---|---|---|---|---|---|---|---|
| Pass | 87 | 89 | 120 | 120 | 137 | 167 | 186 |
| Frame | 8 | 2 | 6 | 28 | 10 | 4 | 3 |
| Along Track | | | | | | | |
| BALTR | 3.00 | 3.08 | 3.00 | 3.07 | 3.30 | 3.30 | 2.12 |
| BALTS | 4.68 | -0.25 | 1.76 | 1.04 | -0.54 | 1.65 | 2.91 |
| TBAT | 7.67 | 3.33 | 4.75 | 4.11 | 3.84 | 4.95 | 5.04 |
| RESL | 104.0 | 126.2 | 121.0 | 123.3 | 129.4 | 120.0 | 121.6 |
| RESH | 120.4 | 195.3 | 167.9 | 181.0 | 188.1 | 164.9 | 162.3 |
| GDRL | 10.1 | 8.6 | 8.9 | 8.3 | 7.6 | 7.7 | 7.7 |
| GDRH | 8.7 | 5.5 | 6.4 | 5.6 | 5.2 | 5.6 | 5.7 |
| Cross-Track | | | | | | | |
| BCTR | 0.86 | 0.88 | 0.85 | 0.88 | 0.97 | 0.98 | 0.64 |
| BCTS | 16.72 | -8.18 | 18.09 | -7.13 | 13.53 | -2.14 | 3.57 |
| TBCT | 17.58 | 9.07 | 18.94 | 8.02 | 14.50 | 3.16 | 4.21 |
| CRESL | 54.7 | 95.6 | 50.9 | 105.1 | 65.6 | 136.5 | 129.2 |
| CRESH | 55.4 | 104.8 | 51.4 | 117.7 | 67.0 | 203.9 | 179.6 |
| CGDRL | 20.7 | 12.4 | 23.5 | 10.5 | 15.2 | 6.8 | 6.9 |
| CGDRH | 20.5 | 11.3 | 23.3 | 9.3 | 14.9 | 4.5 | 5.0 |

Table B-2 — Resolution Predictions for HPL Targets, Aft-Looking Camera, Unit No. 304

| | | | | | | | |
|---|---|---|---|---|---|---|---|
| Target | 121 | 104 | 301 | 120 | 106 | 31 | 302 |
| Pass | 24 | 24 | 154 | 7 | 21 | 39 | 72 |
| Frame | 27 | 65 | 40 | 26 | 66 | 54 | 12 |
| Along Track | | | | | | | |
| BALTR | 2.57 | 2.47 | 1.89 | 2.60 | 2.60 | 2.59 | 2.53 |
| BALTS | -0.01 | -1.14 | 1.38 | 1.49 | -0.65 | 0.45 | -0.18 |
| TBAT | 2.57 | 3.60 | 3.27 | 4.08 | 3.25 | 3.03 | 2.70 |
| RESL | 126.9 | 105.4 | 126.9 | 121.4 | 105.0 | 115.7 | 106.8 |
| RESH | 165.5 | 158.0 | 172.5 | 168.0 | 159.0 | 158.7 | 164.0 |
| GDRL | 8.2 | 9.9 | 8.2 | 8.6 | 9.7 | 8.3 | 9.2 |
| GDRH | 6.3 | 6.6 | 6.0 | 6.2 | 6.4 | 6.1 | 6.0 |
| Cross Track | | | | | | | |
| BCTR | 0.75 | 0.71 | 0.54 | 0.77 | 0.77 | 0.76 | 0.74 |
| BCTS | -4.17 | 13.33 | 11.58 | 10.65 | 10.55 | 10.61 | 11.61 |
| TBCT | 4.92 | 14.04 | 12.12 | 11.42 | 11.32 | 11.38 | 12.35 |
| CRESL | 120.0 | 68.9 | 80.2 | 82.9 | 80.0 | 79.7 | 75.5 |
| CRESH | 149.2 | 70.3 | 80.7 | 85.5 | 85.0 | 85.3 | 78.8 |
| CGDRL | 9.0 | 16.4 | 14.3 | 12.8 | 12.9 | 12.3 | 13.5 |
| CGDRH | 7.2 | 16.1 | 14.2 | 12.4 | 12.2 | 11.5 | 13.0 |

Table B-2 — Resolution Predictions for HPL Targets, Aft-Looking Camera, Unit No. 304 (Cont.)

| | | | | | | |
|---|---|---|---|---|---|---|
| Target | 303 | 105 | 120 | 103 | 80 | 105 |
| Pass | 87 | 89 | 120 | 137 | 167 | 186 |
| Frame | 14 | 8 | 34 | 16 | 10 | 10 |
| Along Track | | | | | | |
| BALTR | 2.36 | 2.37 | 2.46 | 2.61 | 1.65 | 1.32 |
| BALTS | 1.15 | 1.95 | 0.14 | 0.82 | 0.70 | 2.43 |
| TBAT | 3.50 | 4,32 | 2.61 | 3.42 | 2.35 | 3.75 |
| RESL | 105.5 | 122.8 | 128.7 | 107.5 | 128.3 | 130.3 |
| RESH | 159.6 | 157.9 | 173.4 | 174.6 | 174.8 | 185.4 |
| GDRL | 9.6 | 8.8 | 8.0 | 9.3 | 7.3 | 7.2 |
| GDRH | 6.4 | 6.8 | 5.9 | 5.7 | 5.3 | 5.1 |
| Cross Track | | | | | | |
| BCTR | 0.67 | 0.68 | 0.71 | 0.77 | 0.49 | 0.40 |
| BCTS | 13.54 | -6.06 | -5.52 | 11.08 | -0.87 | 2.39 |
| TBCT | 14.21 | 6.74 | 6.22 | 11.85 | 1.36 | 2.78 |
| CRESL | 68.7 | 111.2 | 114.4 | 81.9 | 130.6 | 135.6 |
| CRESH | 69.5 | 127.6 | 133.7 | 82.3 | 173.2 | 212.2 |
| CGDRL | 16.3 | 10.6 | 9.6 | 12.3 | 7.1 | 6.6 |
| CGDRH | 16.1 | 9.2 | 8.2 | 12.2 | 5.4 | 4.2 |

Table B-3 — Average Low Contrast Ground Resolved Distance Versus Photointerpreter Ratings

The average low contrast ground resolved distance is obtained by averaging the ground resolved distances for the forward- and aft-looking cameras in both the along- and cross-track directions. In other words, it is the average of four numbers. Note that the photointerpreter ratings include weather effects which have been eliminated by necessity from the predicted average ground resolved distance.

| Target Number | Pass | Average GRD, feet | Photointerpreter Rating |
|---|---|---|---|
| 120 | 7 | 11.3 | Fair |
| 106 | 21 | 11.7 | Fair |
| 121 | 24 | 8.8 | Fair |
| 104 | 24 | 13.9 | Good |
| 31 | 39 | 10.9 | Good |
| 302 | 72 | 12.1 | Fair |
| 303 | 87 | 14.2 | Fair |
| 105 | 89 | 10.1 | Fair |
| 120 | 120 | 9.1 | Fair |
| 103 | 137 | 11.1 | Poor |
| 301 | 154 | 13.1 | Fair |
| 80 | 167 | 7.2 | Good |
| 105 | 186 | 7.1 | Fair |

NOTE: The following statistics have been computed for the various photointerpreter ratings:

| Photointerpreter Rating | Mean GRD, feet | Standard Deviation, feet |
|---|---|---|
| Good | 10.7 | 2.7 |
| Fair | 13.1 | 2.9 |
| Poor | 17.1 | 4.1 |

These statistics include the photointerpreter ratings and predicted average GRD's of mission 1101.

## Appendix C

## PHOTOGRAPHIC ILLUSTRATIONS

The following two photographs are 40× enlargements of the MIP and corresponding frames from mission 1102.

The next illustration is a series of comparative photomicrographs of the MIP frames from missions 1101 and 1102. Mission 1101 received an MIP rating of 95 and 1102 an MIP rating of 100. The enlargements are approximately 100×. The 1101 performance report indicated that the enlargement was 120×, which is in error. The top photograph shows the same areas as used in a similar comparison from the 1101 mission. The bottom photograph shows some commercial aircraft from the MIP frame. Since the previous comparison used military aircraft (B-52's), an enlargement was made from a different frame on the same pass that took the MIP frame. This is the middle photograph in this series.

~~Handle Via~~
~~Talent-KEYHOLE~~
~~Control System Only~~

~~Handle Via~~
~~Talent-KEYHOLE~~
~~Control System Only~~

[redacted]

TOP SECRET

NO FOREIGN DISSEMINATION

MIP Frame
Mission—1101-2
Pass—D159
Camera—Fwd
Frame—002
Altitude—84 nm
X-Coord—39.0
System—KH-4B
MIP 95

Frame From MIP Pass
Mission—1102-1
Pass—D016
Camera—Fwd
Frame—013
Altitude—88 nm
X-Coord—30.8
System—KH-4B

Frame taken from MIP pass for comparison purposes

MIP Frame
Mission—1102-1
Pass—D016
Camera—Fwd
Frame—022
Altitude—88 nm
X-Coord—26.8
System—KH-4B
MIP 100

100· photomicrographs of comparative frames having MIP ratings of 95 and 100

TOP SECRET

NO FOREIGN DISSEMINATION

HANDLE VIA TALENT-KEYHOLE CONTROL SYSTEM ONLY

## Appendix D

## WEATHER ASSESSMENT

Weather assessment is carried out by using Disic imagery that has corresponding main camera photography. From each corresponding frame, an estimate of clear, clouds, and haze is made. This estimate is the percentage of area that each of the three encompasses in the format.

The haze ratio, being an area weighted percentage of haze in the cloud-free portions of the format, is then determined.

The data in Table D-1 represent the average weather assessment for all of the Disic frames in the first segment of mission 1102 and from passes 081 to 187 in the second segment of mission 1102. The data in Table D-2 is a pass-by-pass weather estimate of the entire 1102 mission. The 02 bucket of the mission is incomplete (beyond pass 187) due to a malfunction of the Disic camera during the latter part of the mission.

In comparing the final averages with those of mission 1101 (refer to Table D-3), it is obvious that the results are quite comparable. Very little difference exists in percent cloud, haze, and clear.

Table D-1 — Weather Estimation Averages for the Entire Panoramic Coverage Portion of the Mission

| Mission | Cloud, percent | Haze, percent | Clear, percent | Haze Ratio |
|---|---|---|---|---|
| 1102-1 | 30.1 | 11.5 | 58.4 | 16.4 |
| 1102-2 | 32.7 | 16.9 | 50.4 | 25.1 |
| Mission average | 31.4 | 14.2 | 54.4 | 20.8 |

Table D-2 — Weather Estimations for the Entire Panoramic Coverage Portion of the Mission

Mission 1102-1

| Rev | Clouds, percent | Haze, percent | Clear, percent | Haze Ratio |
|---|---|---|---|---|
| 001 | 84 | – | 16 | – |
| 005 | 19 | 16 | 65 | 20 |
| 006 | 12 | – | 88 | – |
| 007 | 38 | 14 | 48 | 22 |
| 008 | 1 | – | 99 | – |
| 009 | 36 | – | 64 | – |
| 010 | 27 | 25 | 48 | 34 |
| 011 | – | – | 100 | – |
| 013 | 55 | – | 45 | – |
| 015 | 10 | – | 90 | – |
| 016 | – | – | 100 | – |
| 021 | 39 | 2 | 59 | 3 |
| 022 | 32 | 3 | 65 | 4 |
| 024 | 19 | 1.5 | 79.5 | 1.8 |
| 025 | 6.5 | 56 | 37.5 | 59 |
| 026 | 2 | 44 | 54 | 45 |
| 030 | 52 | 1 | 47 | 2 |
| 032 | – | – | 100 | – |
| 037 | 6 | – | 94 | – |
| 038 | 64 | 10 | 26 | 28 |
| 039 | 11 | 3.5 | 85.5 | 4 |
| 040 | – | – | 100 | – |
| 041 | 15 | – | 85 | – |
| 042 | 13 | – | 87 | – |
| 046 | 57 | 17 | 26 | 40 |
| 047 | 60 | 3 | 37 | 7.5 |
| 048 | 55 | – | 45 | – |
| 053 | 39 | 15 | 46 | 25 |
| 054 | 40 | 5 | 55 | 8.3 |
| 055 | 75 | – | 25 | – |
| 056 | 28.5 | 26 | 45 | 37 |
| 057 | – | – | – | – |
| 058 | 100 | – | – | – |
| 059 | 10 | 90 | – | 100 |
| 064 | 5 | 95 | – | 100 |
| 071 | 34 | 1.5 | 64.5 | 2 |
| 072 | 54 | – | 46 | – |
| 074 | 88 | 7 | 5 | 58 |
| 075 | – | 10 | 90 | 10 |
| 079 | – | – | 100 | – |
| Average | 30.1 | 11.5 | 58.4 | 29.1 |

Mission 1102-2

| Rev | Clouds, percent | Haze, percent | Clear, percent | Haze Ratio |
|---|---|---|---|---|
| 081 | 100 | – | – | |
| 087 | 58 | 7 | 35 | 17 |
| 089 | 28 | 10 | 62 | 14 |
| 090 | 4 | 2 | 94 | 2 |
| 097 | – | – | 100 | . |
| 102 | 3 | 1 | 96 | 1 |
| 103 | 22 | 38 | 40 | 49 |
| 104 | – | 40 | 60 | 40 |
| 105 | 70 | 27 | 3 | 90 |
| 106 | 32 | 1 | 67 | 1 |
| 107 | 11 | 68 | 21 | 76 |
| 108 | 16.5 | 24.5 | 59 | 29 |
| 111 | 50 | – | 50 | – |
| 113 | 36 | 14 | 50 | 21 |
| 118 | 25 | – | 75 | – |
| 119 | 13 | 6 | 81 | 7 |
| 120 | 3.5 | 1 | 95.5 | 1 |
| 122 | 3 | 23 | 74 | 24 |
| 129 | 45 | 2 | 53 | 3 |
| 134 | – | – | – | – |
| 135 | 13 | 22 | 65 | 25 |
| 136 | 36 | 11 | 53 | 17 |
| 137 | 32 | 27 | 41 | 39 |
| 138 | 5.5 | 16 | 78.5 | 16 |
| 139 | 100 | – | – | – |
| 142 | 11 | 6 | 83 | 6.7 |
| 148 | – | – | – | – |
| 152 | 2 | – | 98 | – |
| 154 | 87.5 | 8.5 | 4 | 68 |
| 155 | 20 | 80 | – | 100 |
| 156 | 7 | 45 | 48 | 48 |
| 158 | 7 | 3 | 90 | 3 |
| 161 | 100 | – | – | – |
| 167 | – | – | – | – |
| 170 | 3 | 64 | 33 | 66 |
| 171 | 80 | 4 | 16 | 20 |
| 172 | 27 | 60 | 13 | 82 |
| 176 | 63.5 | 6.5 | 30 | 18 |
| 178 | – | – | – | – |
| 182 | 50 | – | 50 | – |
| 184 | 40.5 | 6.5 | 53 | 10 |
| 186 | 20 | – | 80 | – |
| 187 | 49 | 36 | 15 | 70 |
| Average | 32.7 | 16.9 | 50.4 | 32.1 |

| | | |
|---|---|---|
| **Haze ratio (all frames)** | **1102-1** | **16.4** |
| | **1102-2** | **25.1** |
| | **Average** | **20.8** |
| **Haze Ratio (only frames with haze)** | **1102-1** | **29.1** |
| | **1102-2** | **32.1** |
| | **Average** | **30.6** |

Table D-3 — Comparison of Final Averages Obtained From Missions 1101 and 1102

| Mission | Cloud, percent | Haze, percent | Clear, percent | Haze Ratio | NPIC Evaluation, percent |
|---|---|---|---|---|---|
| 1102 1 | 30.1 | 11.5 | 58.4 | 16.4 | 70 clear |
| 1102-2 | 32.7 | 16.9 | 50.4 | 25.1 | 75 clear |
| 1101-1 | 33 | 14.5 | 52.5 | 21.6 | 65 clear |
| 1101-2 | 33 | 8.5 | 58.5 | 12.7 | 70 clear |